Evaluation of the 5-ethynyl-1,3,3-trimethyl-3*H*-indole ligand for molecular materials applications.

David Jago,[1] David Costa Milan,[2] Alexandre N. Sobolev,[3] Simon J. Higgins,[2] Andrea Vezzoli,[2] Richard J. Nichols,[2] George A. Koutsantonis[1,]*

[1] Chemistry, School of Molecular Sciences, The University of Western Australia, Crawley, WA, 6009, Australia

[2] Department of Chemistry, University of Liverpool, Liverpool, UK

[3] Centre for Microscopy, Characterisation and Analysis, The University of Western Australia, Crawley, WA, 6009, Australia

Abstract

The modification of conjugated organic compounds with organometallic moieties allows for the modulation of the electronic and optoelectronic properties of such compounds and lend themselves to a variety of material applications. The organometallic complexes [{M(Cp')$(L)_n$}] (M = Ru or Fe, Cp' = Cp or Cp*, L = PPh_3 or dppe) and [$M(L)_n$] (M = Ru, L = dppe, or $P(OEt)_3$, or M = Pt, L = PEt_3, PPh_3 or PCy_3) modified with a 5-ethynyl-1,3,3-trimethyl-3H-indole ligand were prepared and characterized by NMR spectroscopy, IR and single-crystal X-ray diffraction. Cyclic voltammetry and IR spectroelectrochemistry of the ruthenium systems showed a single electron oxidation localized over the M-CC-Aryl moiety. The N-heteroatom of the indole ligand showed

Lewis-base properties and was able to extract a proton from a vinylidene intermediate as well as coordinate to Cu(I). Examples from the wire-like compounds were also studied by single-molecule break junction experiments but molecular junction formation was not observed. This is most likely attributed to the binding characteristics of the substituted terminal indole groups used here to the gold contacts.

Introduction

The ability to incorporate molecules as functional building blocks for molecular systems has gained the attention of chemists for the best part of a century. Organic π-conjugated compounds possess properties that lend themselves to various electronic and optoelectronic materials.[1-3] Incorporating organometallic fragments allows for the fine-tuning of electronic structure and function in organic molecules.[4] The capacity to modulate the properties of the ligand has seen metal complexes applying to a variety of applications including molecular electronics, non-linear optical materials,[5] surface-based catalysis,[6] photovoltaics,[7] and luminescent and responsive materials.[8]

The design and optimisation of new materials based on organometallic complexes relies on the exploration of new metal complexes and the study of their chemical, physical and optoelectronic features. N-heterocyclic aromatic compounds are used ubiquitously as σ-donor ligands in inorganic chemistry, particularly pyridine-based ligands, which are used to construct large metal-organic frameworks and have gained interest from a variety of fields.[9] In addition, analogies between coordination and molecular-surface interactions provide a basis for motif testing for binding groups in large area ensembles and molecular junctions.[10] Indole and indole derivatives are found both in nature and pharmacology.[11-13] In particular, the 3*H*-indole is an important

structural motif and has been used as a scaffold to form other indoline alkaloids.[12, 14] Further functionalisation of the 3*H*-indole moiety is an attractive venture for expanding its synthetic facility.

Metal alkynyl complexes have become building blocks for the synthesis and study of ligand bridged polymetallic systems.[15, 16] They are ideal candidates for studying mixed-valence systems and other intramolecular electron-transfer processes. In particular, the complexes containing the d^8 and d^{10} metal centres are well versed organometallic systems with the ability to tune the oxidation site using different metals and ancillary ligands, which can moderate the opto-electronic properties of the ligand.[8, 17, 18]

We have previously investigated the moderation of electro-optical properties of pyridyl and bipyridyl moieties into σ-alkynyl, vinylidene and allenylidene organometallic complexes.[19-23] Herein, the synthesis of a series of organometallic complexes derived from the 5-ethynyl-*3*H-indole moiety is reported and their physical and chemical properties are described.

Results and Discussion

Synthesis

The 3*H*-indole ligand **2** was obtained in high yield by the KOH promoted desilylation of **1** (Scheme 1). The ethene **3** was also obtained from this reaction. The mechanism for the formation of **3** is not well understood.

A similar ethene compound from the reaction of an alkyllithium reagent and a 3*H*-indole has been reported and was proposed to from by a radical mechanism (Scheme S1).[24] ESR spectroscopy has confirmed the presence of a radical intermediate from the reaction of methylmagnesium iodide or organolithium reagents and a 3*H*-indole.[24, 25] Alternative oxidation mechanisms are proposed in the absence of such alkyl reagents in this current study (Scheme S2).

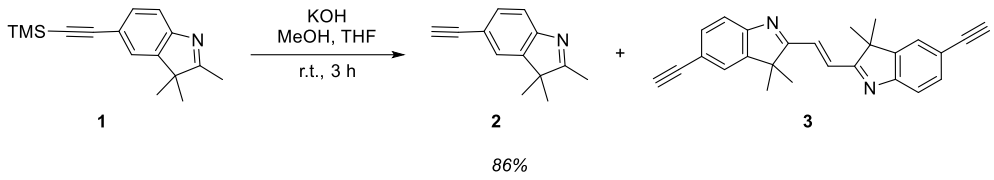

Scheme 1 Synthesis of 5-ethynyl-2,3,3-trimethyl-3*H*-indole **2**.

Following the oxidation of **2** to the aldehyde, in a manner similar to that in the literature,[26-28] an aldol condensation with another molecule of **2** and the elimination of water gives the ethene dimer **3**. The propensity of molecules similar to **2** to undergo aldol condensation is known.[29] Alternatively, the oxidation of **2** to the N-oxide is also plausible. As similar self-condensation of indolium salts has previously been observed,[30, 31] which involves the activation of the indole to the N-oxide for further reactions such as the reaction with another molecule of 3*H*-indole. Subsequent deprotonation and elimination of water yields the dimeric indole molecule. Schemes for these proposed mechanisms are shown in the supporting information.

The ^{1}H NMR spectrum of **2** shows a resonance assigned to the terminal alkyne proton at 3.07 ppm. Sharp absorptions at 3176 (ν(CH)) and 2099 (ν(C≡C)) cm^{-1} in the IR spectrum further evinced the terminal alkyne functional group. Compound **3** is fluorescent under UV light. The alkene bridge was assigned to the singlet at 3.07 and 128.51 ppm in the ^{1}H and ^{13}C NMR spectra, respectively. A weak absorption at 1607 cm^{-1} in the IR provided further evidence for the alkene bridge (ν(C=C)). The APCI mass spectrum showed a peak at *m/z* 363.1851 consistent with the molecular ion. Single-crystal X-ray diffraction studies confirmed the connectivity of **2** and **3**.

The half-sandwich monometallic σ-alkynyl complexes were synthesised using established or slightly modified literature methodologies. The complexes **4** to **7** were synthesised by the vinylidene route (Scheme 2).[32] The appropriate half-sandwich ruthenium or iron halides and **2** were refluxed in methanol with NH_4PF_6 present to produce a vinylidene intermediate. After the

reaction had cooled to room temperature, the vinylidene species was then deprotonated by carefully adding 1,8-diazabicycloundec-7-ene (DBU) and allowing the mixture to be left undisturbed overnight. The slow diffusion of DBU over a long period afforded well-formed crystals of the targeted complexes. Copper-assisted transmetallation[33] of $Ru(CO)_2(Cp)Cl$ and **2** in THF and NEt_3 afforded **8** in good yield (Scheme 2), while complex **9** was synthesised in a basic methanolic solution containing **2** and the gold chloride precursor, PPh_3AuCl (Scheme 2).[34] Both **8** and **9** showed light sensitivity. The gold complex is of interest due to its potential use as transmetallation reagent and catalyst.[35-37]

The ruthenium complexes **4** and **5** showed absorptions at *ca*. 2060 cm^{-1} in their IR spectra assigned to the alkynyl functional group. This assigned ν(C≡C) absorption appeared at a slightly lower wavenumber, *ca*. 2050 cm^{-1}, for the iron complexes **6** and **7**. Comparatively, the alkynyl stretch for **8** was assigned to the IR absorption at 2119 cm^{-1}. Strong absorbances for the symmetric and asymmetric carbonyl stretches for **8** were assigned to the IR bands at 2035 and 1994 cm^{-1}, respectively.

A single peak in the ^{31}P NMR spectrum for **4** to **7** and **9** further evinced the synthesis of the single metal σ-alkynyl complexes. Resonances for the respective cyclopentadienyl ligands were assigned to the peaks δ 4.51 (**4**), 1.68 (**5**), 1.56 (**6**), 4.32 (**7**), 5.48 (**8**). Resonances for the cyclopentadienyl and phosphine ligands are within the typical range of half-sandwich ruthenium and iron complexes.[20, 35, 38, 39]

The ^{1}H and ^{13}C NMR spectra contained resonances consistent with the indole ligand for all complexes. Figure S1 shows the general atom numbering and labelling for the indole and phosphine ligands of the complexes. In general, resonances for Cα, Cβ and C5 are deshielded upon the metal-carbon bond formation of the free ligand. The extent of this deshielding is dependent on

the electron density of the metal-centre.[40] Peaks for the Cα carbon in **4**, (δ 113.8) **5** (δ 127.1), **7** (δ 122.3 ppm) and **8** (δ 81.3 ppm) and the Cβ carbon in **4** (δ 116.1 ppm), **5** (δ 111.4 ppm), **6** (δ 121.1), **7** (δ 122.7) and **8** (δ 111.0) show close agreement to expected resonances.[20, 41] The signals for the Cα for the complexes **4** – **7** appear as triplets due to coupling to the phosphorus ligand on the metal centre. The peak for Cα in complex **9** appeared as a doublet at δ 135.8 with a J_{CP} coupling of 146 Hz, whilst the peak for Cβ appears at δ 104.1 with a J_{CP} coupling of 26 Hz. The chemical shifts and coupling constants are similar to previously synthesised gold(I) alkynyl complexes.[34] The observation of these alkynyl carbons is in contrast to a previous report that suggests these analogous resonances were not observed as a consequence of quadrupolar broadening and quenching in those gold type complexes.[42]

The ES mass spectra of the complexes **4** to **9** showed ions consistent with a $[M+H]^+$ species, except for **6**, which showed a peak assigned to the $[M]^+$ species. In addition, the mass spectra of complexes **4**, **5**, and **7** contained an ion consistent with a $[M+2H]^{2+}$ species. Whereas, the mass spectrum of complex **5** also showed an ion at *m/z* 663, consistent with the oxidative cleavage of the alkyne ligand to give the carbonyl cation complex $[Ru(dppe)(Cp^*)CO]^+$.[43] Most complexes also showed fragmentation consistent with the loss of the alkyne ligand and incomplete desolvation. The spectrum of gold complex **9** also exhibited an ion at *m/z* 721 for the $[Au(PPh_3)_2]^+$ species also seen in previous studies.[42]

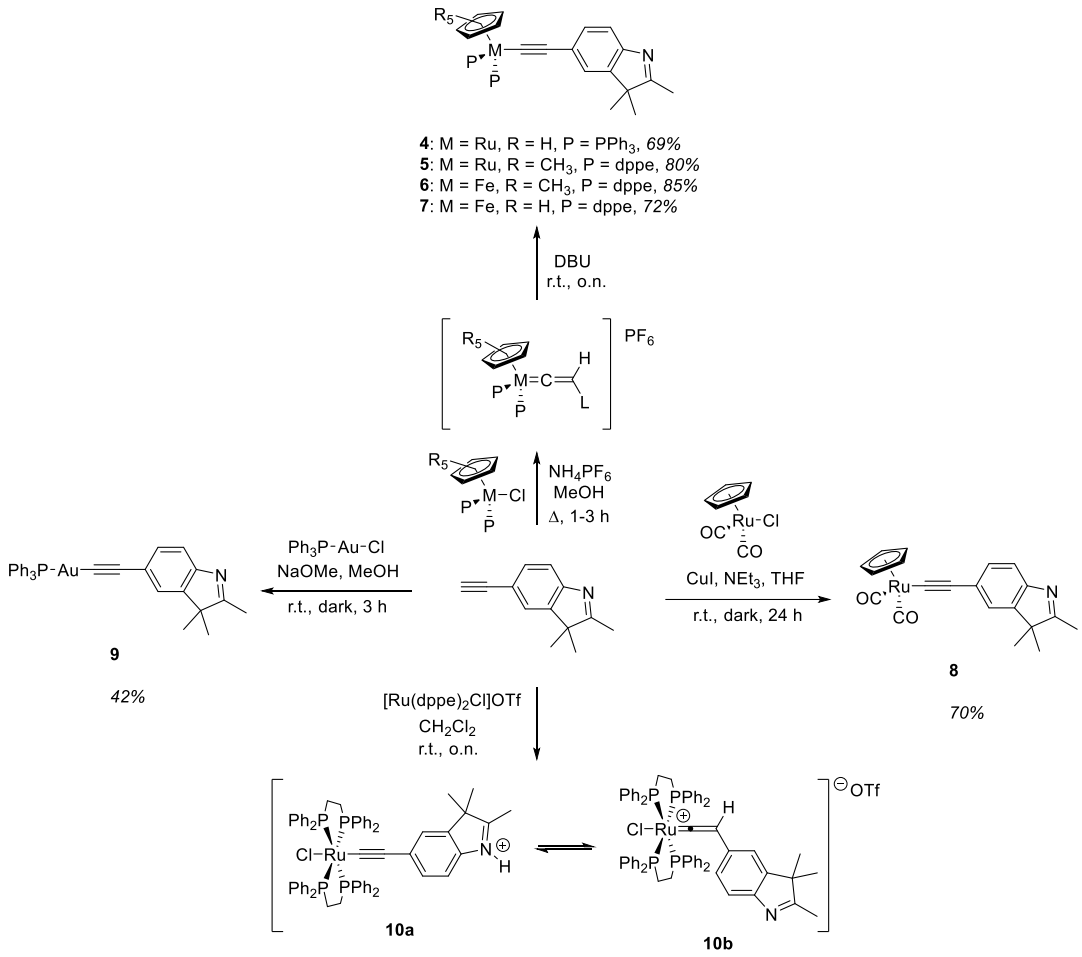

Scheme 2 Preparation of the complexes **4**–**9** and **10a/b**.

The synthesis of the alkynyl complex of **2** containing the $[Ru(dppe)_2Cl]^+$ moiety by a number of alternative, established literature procedures was unsuccessful.[44] However, the reaction of $[Ru(dppe)_2Cl]OTf$ and **2** afforded a mixture of complexes **10a** and **10b**, as evinced by spectroscopic data. We suggest that the basicity of the nitrogen on the indole ligand can deprotonate the intermediate vinylidene species; however, singlet peaks in ^{31}P NMR spectrum at *ca*. 48 and 37 ppm suggest two *trans* configurations are in equilibrium (Scheme 5).[45] This basic proligand effect has been seen in the syntheses of complexes from 5-ethynyl-2,2′-bipyridine using both the $Ru(dppe)_2Cl$ and $RuCp(PPh_3)_2$ moieties.[19, 45] Similar effects have been noted in the

formation of alkynyl complexes from $Ru(dppe)_2Cl_2$ and 4-ethynylaniline,[44] but not with the half-sandwich analogues using the Ru(dppe)(Cp*) moiety.[46] Contrarily, the syntheses of ruthenium pyridyl alkynyl complexes also report this deprotonation when the alkynyl is formed from $RuCp(PPh_3)_2$ halides,[47] but not $Ru(dppm)_2Cl_2$.[48] The ^{19}F NMR spectrum was consistent with the presence of the triflate anion. The ES mass spectrum showed a peak at *m/z* 1121 consistent with $[M\text{-}Cl+MeCN]^+$ species. A presumed impurity, unassigned, was seen at 41 ppm in the ^{31}P NMR and could not be removed by further purification steps. Attempts to deprotonate **10a**/**10b** resulted in mixtures of decomposition and oxidation products as evinced by the numerous peaks observed in the ^{31}P NMR spectra obtained.

The cross-coupling of **2** with 1,4-diiodobenzene in NEt_3 gave **11** (Scheme 3). The ^1H NMR spectrum shows resonances consistent with the geminal methyl groups and imine methyl group at δ 1.32 and 2.30, respectively. The 1,4-substituted benzene and indole are assigned to a multiplet at δ 7.46 - 7.50 in the ^1H NMR spectrum. The ^{13}C NMR shows peaks assigned to the alkynyl carbons at δ 91.9 and 89.1 ppm, shifted downfield from the parent alkyne. The alkynyl bond is also evinced by a band at 2203 cm^{-1} in the IR spectrum. Mass spectroscopy (APCI) shows a peak consistent with the protonated molecular ion at *m/z* 441.2338.

Access to the platinum metal complexes trans-$[Pt(L)_2(PR_3)_2]\}$, where L = CC-2,3,3-trimethyl-3*H*-indole; and, R = Et (**12**), Ph (**13**), or Cy (**16**) (Scheme 3) was achieved by CuI catalysed dehydrohalogenation of $Pt(PR_3)_2Cl_2$ and **2** in the presence of an amine base.[49] While the use of *cis*-$Pt(PR_3)_2Cl_2$ conserves the *cis*-orientation of the complex,[50, 51] however, heating at reflux allows access to the more thermodynamically stable *trans* isomer.

Spectral characteristics of **12** and **13** are comparable to other bis-alkynyl Pt(II) complexes.[49] The ^{31}P NMR spectrum of **12** and **13** show a single resonance (with ^{195}Pt satellites) at δ 11.62 and

19.18, respectively, affirming a *trans* orientation of the phosphine ligands. Resonances in the ^{1}H NMR spectra for the alkyl groups in the triethylphosphines in **12** and phenyl groups in the triphenylphosphines in **13** are assigned to signals at δ 2.17-2.20 (CH_2) and 1.20 – 1.27 (CH_3), and δ 7.40 – 7.84 (30H), respectively. The ^{1}H NMR spectrum also shows singlets consistent with the geminal methyl groups and imine methyl group of the alkynyl indoles in both Pt-complexes. The ^{13}C NMR spectrum shows resonances assigned to the Cα and Cβ alkynyl carbons at δ 107.4 and 109.8, respectively, in **12**. These alkynyl signals for **13** appear at δ 118.8 and 113.7. The IR spectrum of **12** shows a band at 2099 cm^{-1} also affirming an alkynyl ligand. The ν(C≡C) is assigned to an absorption at 2105 cm^{-1} in the IR spectrum of **13**. The HRMS contained peaks consistent with the protonated molecular ion at *m/z* 796.3510 and 1084.3472 for **12** (ES) and **13** (APCI), respectively.

In the synthesis of **12**, extraction of the reaction residue with benzene and subsequent recrystallisation gave the coordination complex **12b** (Figure S8). The complex is a polymeric compound consisting of **12** and CuI, with coordination at the nitrogen of the indole ligand. This compound's connectivity was affirmed by single-crystal X-ray diffraction studies (Figure S9). Both ^{1}H and ^{31}P NMR spectra were unremarkable compared to the parent **12**. Examples of coordination complexes of 3*H*-indoles are rare with only a few iridium, platinum and gold complexes reported.[52-54]

The complex trans-[$Pt(PCy_3)_2Cl_2$]} **14** has previously been synthesised by the reaction of [$Pt(COD)Cl_2$] with PCy_3 in THF.[55] Adapting the synthetic procedure for cis-/trans-$PtCl_2(PEt_3)_2$,[56] the reaction of commercially available $(NH_4)_2PtCl_4$ and PCy_3 in toluene and water gives **14** in 83% yield (Scheme 3). Formation of the trans orientation is evinced by a single peak

at δ 17.18 (J_{PPt} = 2398 Hz) in the $^{31}P\{^{1}H\}$ NMR spectrum. The increased steric bulk of the PCy_3 hinders formation of the *cis* orientation.

Due to the scarcity of bis-alkynyl complexes of the type *trans*-[$Pt(PCy_3)_2(CC\text{-}Ar)_2$], a brief optimisation synthesis of trans-[$Pt(PCy_3)_2(CC\text{-}C_6H_5)_2$] **15** was undertaken. The reaction of **14** and phenylacetylene in the presence of CuI, triethylamine and co-solvent $CHCl_3$ gives **15** in 59% yield (Scheme 3). The co-solvent was required due to solubility issues of **14** in neat amine solutions. Other co-solvents tested were THF and CH_2Cl_2. The steric bulk of the PCy_3 ancillary ligands renders this reaction sluggish even at elevated temperatures. This observation is mirrored in a study that found only 50% conversion (30% isolated yield) to the *bis*-alkynyl Pt complexes *trans*-[$Pt(PCy_3)_2(CC\text{-}C_6H_4SAc)_2$] after 4 days at 60 °C by similar methodology.[57] The ^{31}P NMR spectrum of **15** shows a single peak at δ 24.06 (J_{PPt} = 2408 Hz). These conditions were employed to synthesise the Pt complex **16**; however, this reaction took 21 days to complete and was low yielding (Scheme 3)

A peak at δ 23.22 (J_{PPt} = 2424 Hz) in the ^{31}P NMR spectrum for **16** evinced a single *trans* orientated complex. The ^{1}H NMR spectrum showed three resonances assigned to the aryl protons on the 3*H*-indole ligand at δ 7.34, 7.21 and 7.14. Broad unresolved resonances in the range δ 1.20 – 2.89 were assigned to signals from the cyclohexyl groups and the methyl groups on the 3*H*-indole. The ES mass spectrum shows a peak consistent with the protonated molecular ion at *m/z* 1120.6332.

The ruthenium complex **17** was synthesised by the reaction of [$RuCl(dppe)_2$]OTf with excess **2**, in the presence of KO^{t}Bu (Scheme 3). This reaction is analogous to established methodology using $NaPF_6$ and NEt_3;[44, 58-60] however, the base and halide abstracting reagent are combined as a single compound, KO^{t}Bu. Another ruthenium complex **18** was synthesised by reaction of *trans*-

$[RuCl_2(P(OEt)_3)_4]$ with **2**, KPF_6 and HN^iPr_2 in ethanol for 8 weeks (Scheme 3). The low yield is comparable to that of previous bis(alkynyl) complexes synthesised by this method.[61] Whilst the use of lithium alkynyl species can be used to obtain this type of alkynyl complexes in low to moderate yields,[62] a simple extraction and crystallisation workup makes this method favourable.

The IR spectra of complexes of **17** and **18** showed absorptions assigned to ν(C≡C) bands at 2048 and 2088 cm^{-1}, respectively. Singlets in the ^{31}P NMR spectrum of both complexes support *trans* arrangement of the ligands and are comparable to similar complexes.[61, 63] The ^1H NMR spectrum of **17** shows a slight upfield shift of the assigned signals for the geminal methyl groups at δ 1.12 ppm and the imine methyl group at δ 2.03 ppm compared to free ligand **2**. This upfield shift was reciprocated in complex **18**, but not to the same extent. Resonances assigned to the ancillary phosphine ligands in **17** were observed between δ 6.94 – 7.76 and 2.56 (m, 8H, $PPh_2CH_2CH_2PPh_2$) in the ^1H NMR spectrum. Resonances assigned to the ethyl fragments on the phosphite groups for **18** were assigned to the quartet at δ 4.33 (CH_2) and the triplet at δ 1.21 (CH_3) (J = 7.2 Hz) in the ^1H NMR spectrum. The mass spectrum (APCI for **17**, ES for **18**) of both complexes show fragmentation consistent with the loss of one alkynyl ligand. In addition, **17** also showed a peak consistent with the protonated molecular ion at *m/z* 1263.3789 in the mass spectrum.

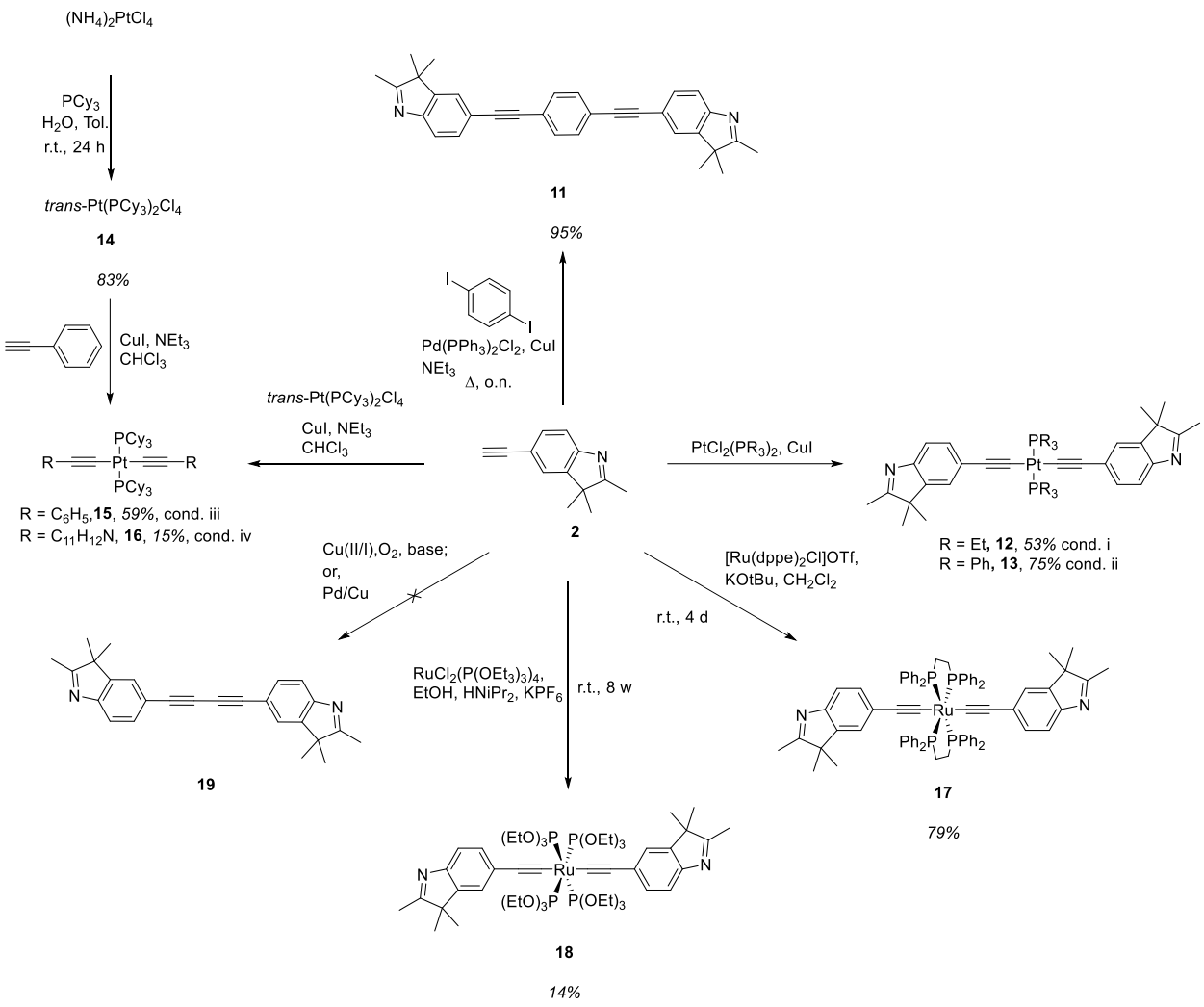

Scheme 3 Preparation of the compounds **11**–**18**. Conditions, i. NEt_3, 70°C, 19 h; ii. HN^iPr_2, reflux, 3 h, iii. 60°C, 11 d; iv, 55°C, 21 d.

Numerous attempts to synthesise the buta-1,3-diyne bridged putative molecular wire **19** were unsuccessful (Scheme 3). These compounds serve as candidates for applications in molecular electronics, supramolecular chemistry, optoelectronics, and conjugated polymers.[64-66] Hay,[67] Eglington,[68] Glaser,[69] and Pd-type[70] coupling reactions failed to produce the homo-coupled product, returning starting material or unidentified decomposed species.

Electronic Spectroscopy

The UV-vis spectra obtained for complexes **4**–**7** all displayed similar features (Figure 1). All complexes show a MLCT just below 400 nm[40] as well as an a higher energy transition below 300 nm. This higher energy band is assigned to a π-π* (IL) transition.

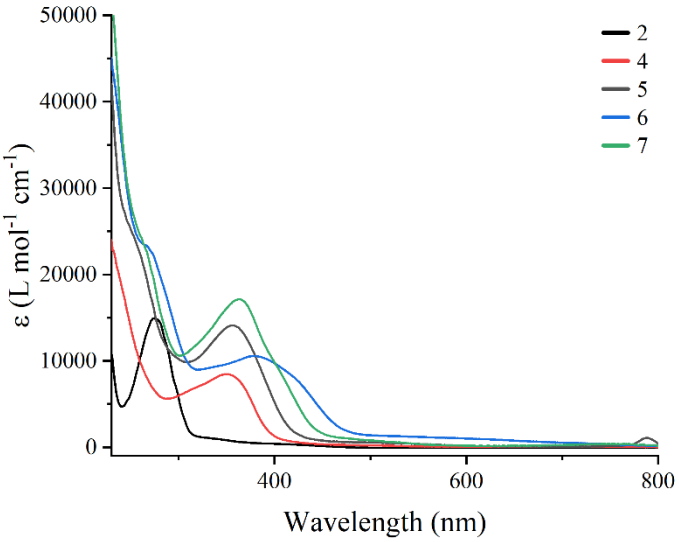

Figure 1 UV-vis Spectra of compound **2**, and complexes **4**–**7** in CH_2Cl_2.

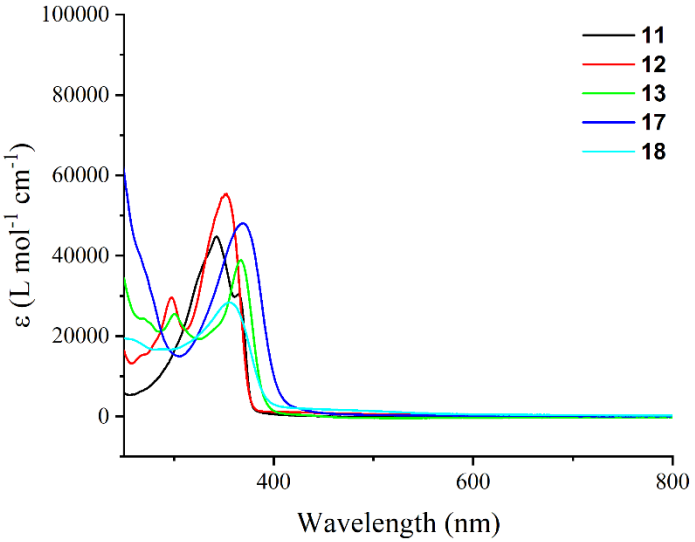

Figure 2 UV-vis spectra of compound **11**, and complexes **12**, **13**, **17** and **18** in CH_2Cl_2.

The UV-vis spectra of **11** and the complexes **12**, **13**, **17**, and **18** are shown in Figure 2. Compound **11** shows absorption maxima at 343 and 365 nm. The platinum complexes **12** and **13** show a high energy transition at *ca.* 300 nm and a lower energy transition between 350 and 370 nm. The lower energy transition has been assigned as a LMCT from the π(CCAr) to the mixed π(CCAr)* and metal p-orbitals.[57, 71, 72] The ruthenium alkynyl complexes also exhibited a band of similar intensity between 350 and 370 nm, with a very intense band appearing below 300 nm for complex **17**. The lower energy band for these and similar complexes has been assigned as a MLCT and the high energy transition as an IL charge transfer band.[73-76]

Molecular Structures

The molecular structures of several compounds in this study have been determined using single-crystal X-ray diffraction studies. Plots are shown in the figures below, and Table 1 and Table 2 shows selected bond lengths and angles.

The organic ligand **2** crystallised with two crystallographically-distinct molecules in the unit cell (Figure 3). The distinction between the molecules lies along with the clockwise or anticlockwise rotation along the C7-C7a-N1-C2 dihedral angle. However, given the near-planar arrangement of both molecules in the unit cell, this is unremarkable. This phenomenon has been reported in a recent communication.[77] The ethene compound **3** shows elongation of the N1-C2 bond and shortening of the C2-C21 bond consistent with conjugation along the N1-C2-C21-C22-N2 backbone (Supporting information Figure S6). Both indole rings are essentially coplanar and arranged in an antiperiplanar arrangement.

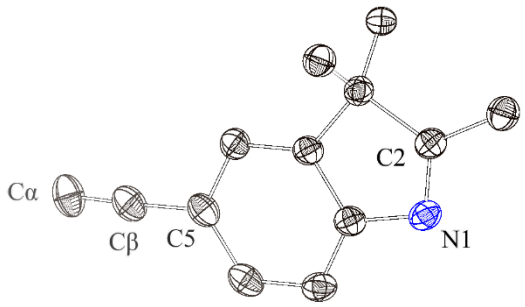

Figure 3. ORTEP representation of **2**, and atom numbering scheme. Ellipsoids at the 50% probability level. Hydrogens removed for clarity.

Complex **4** crystallised with two CH_2Cl_2 solvate molecules (Figure 4). One of the solvent molecules was modelled as disordered over one site. The additional solvate was hydrogen-bonded between the C21-H21--Cl and $CHCl_2$-H--N1 with distances of 3.68(1) and 3.54(2) Å, respectively, between the donor and acceptor atoms.

The bond lengths and angles around the metal core of the complexes are consistent with previously reported analogous alkynyl complexes.[20, 39, 41] Bond lengths along the Ru-CC-C5 are not significantly different between complex **4** and **5** (Figure 4). A smaller Fe-C bond length in **6** (Figure 4) can be ascribed to smaller atomic radii.[17] The usual linear arrangement along the ruthenium alkynyl backbone is observed with a maximum deviation from 180° observed for **5** by -5.7°. The angles subtended by the phosphine atoms at the ruthenium atoms exemplify the pseudo-octahedral environment around the metal centres. The P-Ru-P angles are 100.27(7)° for the *bis* triphenylphosphine and 83.36(2)° for the dppe. The shorter Ru-P bonds in **5** are consistent with the increased electron density at the metal centre, favouring back-bonding with the phosphine ligands. Bond lengths and angles for complex **8** (Figure 4) are also unremarkable compared to similar complexes.

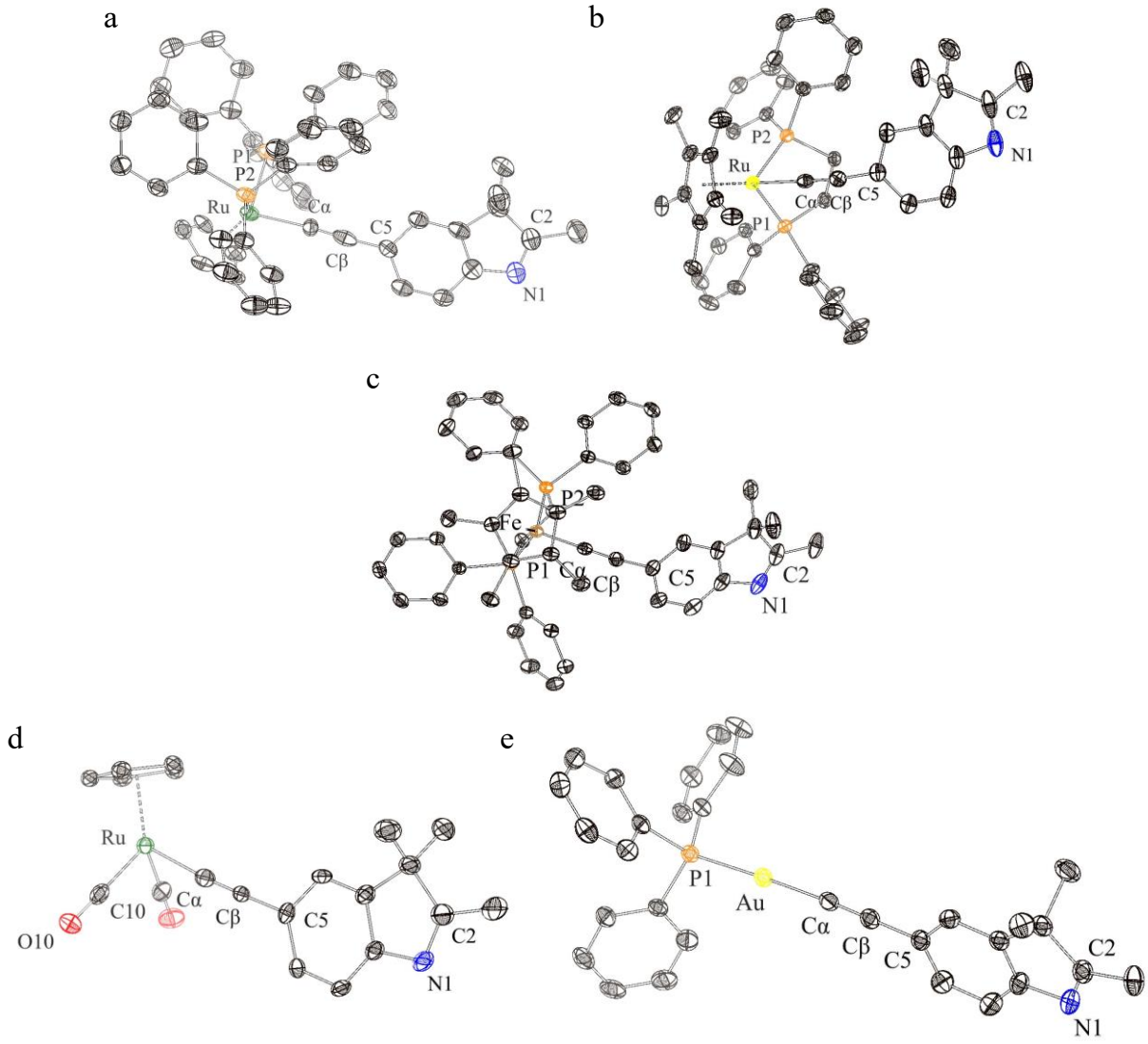

Figure 4. ORTEP representations of (a) **4**, (b) **5**, (c) **6**, (d) **8** and (e) **9**, and atom numbering scheme. Ellipsoids at the 50% probability level. Hydrogens and solvates removed for clarity where appropriate.

The Au-C and CC bond lengths, and the bond angles about the P-A-CC chain for **9** (Figure 4) are within the ranges for reported Au(I) alkynyl complexes.[34, 42, 78-81] A near-linear arrangement of alkynyl and phosphine ligands at the gold centre is observed. The slightly increased deviation from linearity at the Au-CC moiety has been associated with crystal packing forces.[79, 81]

The relative orientation of the indole ring is influenced by the steric encumbrance of the ancillary ligands in the solid-state. The torsion angle between the centroid of the cyclopentadienyl ligand, metal atom, and the C5 and C4 atoms is used to highlight the orientation of the indole ring (Figure S10). In complex **8**, the indole ring lies perpendicular to the cyclopentadienyl ligand. In complex **4**, introducing the bulky triphenylphosphine ligands cause the indole to rotate close to 180°. Complex **5**, the indole ligand lies in the plane of the cyclopentadienyl ligand due to the increased bulk of the permethylated Cp ligand and less sterically demanding dppe. Similar parallel conformation for functionalised ethynyl aryl rings in ruthenium σ-alkynyl complexes have been reported.[46] This sentiment is also reflected in the orientation of the indole ligand in complex **6**.

Table 1. Selected bond lengths (Å) and bond and torsion angles (°) from the crystallographically determined structures

	M-P1	M-P2	M-Cα	Cα-Cβ	Cβ-C5	N1-C2	C21-C22	M-Cα-Cβ	Cα-Cβ-C5	P-M-P	θ	θ′
2				1.198(4)	1.439(4)	1.289(3)			178.0(3)			
3				1.199(1)	1.438(1)	1.312(1)	1.352(1)		177.5(1)			175.4(1)
4	2.293(2)	2.281(2)	2.034(6)	1.161(10)	1.444(14)	1.277(10)		174.4(6)	176.2(8)	100.27(7)	173.18	
5	2.2578(7)	2.2556(6)	2.012(2)	1.218(3)	1.442(3)	1.280(4)		178.3(2)	174.3(2)	83.36(2)	72.78	
6	2.1795(6)	2.1741(5)	1.900(1)	1.225(2)	1.437(2)	1.286(3)		178.3(1)	174.1(2)	85.89(2)	69.72	
8	1.867[a]	1.146(5)[a]	2.033	1.182	1.461	1.278		175.8	179.3	91.9	0	
9	2.2717(7)		2.006(3)	1.208(4)	1.438(4)	1.287(4)		173.2(2)	176.0(2)	177.87(7)[b]		

[a]Ru-C. [b]P-Au-Cα. θ is the dihedral angle between the centroid of the Cp ring and the aryl plane for the alkynyl ligand for the half-sandwich complexes. θ′ is the torison angle between the two indoline rings

Compound **11** (Figure 6) mirrors the solid-state structure of the recently reported 1,4-bis(5-ethynyl-3,3-dimethyl-2,3-dihydrobenzo[*b*]thiophenyl)benzene.[60] The central phenyl ring possesses an inversion centre tilted by 35.0(3)° from the outer indole ring. Simpler phenylene-ethynylene structures seem to adopt a more coplanar orientation in the solid-state.[60, 82] Inter-molecular hydrogen bonding between the N1 and imine methyl group dominate the crystal packing.

Solid-state structures showed the expected square planar geometry around the metal centre in the platinum complexes **12**, **13**, and **16** (Figure 6) as well as **15** (Figure S7) All complexes except **15**, which exhibits a slight distortion, sit on crystallographic inversion centres and have similar bond angles that deviate only slightly from idealised square planar geometry. Hydrogen bonding between N1 and methanol solvent dominates the crystal lattice of **16**. The M-P bond length is shorter in **12** compared to the other Pt complexes in this study. In general, characteristic bonds lengths and angles along the metal-alkyne fragment were unremarkable and were within the range reported in the literature.[83-88]

Complex **17** possessed a centre of inversion about the ruthenium centre (Figure 6). The plane of the aryl-ethynyl rings of the indole lies between the dppe bidentate ligands. The angle between the plane of the arylethynyl ligand and the plane bisecting the dppe ligand, θ, as described recently,[63] is 76.8°. In this orientation, there is a better overlap of the ligand π-system with the metal centre. All other interatomic parameters are not significantly different from previously described trans-Ru bis(alkynyl) complexes.

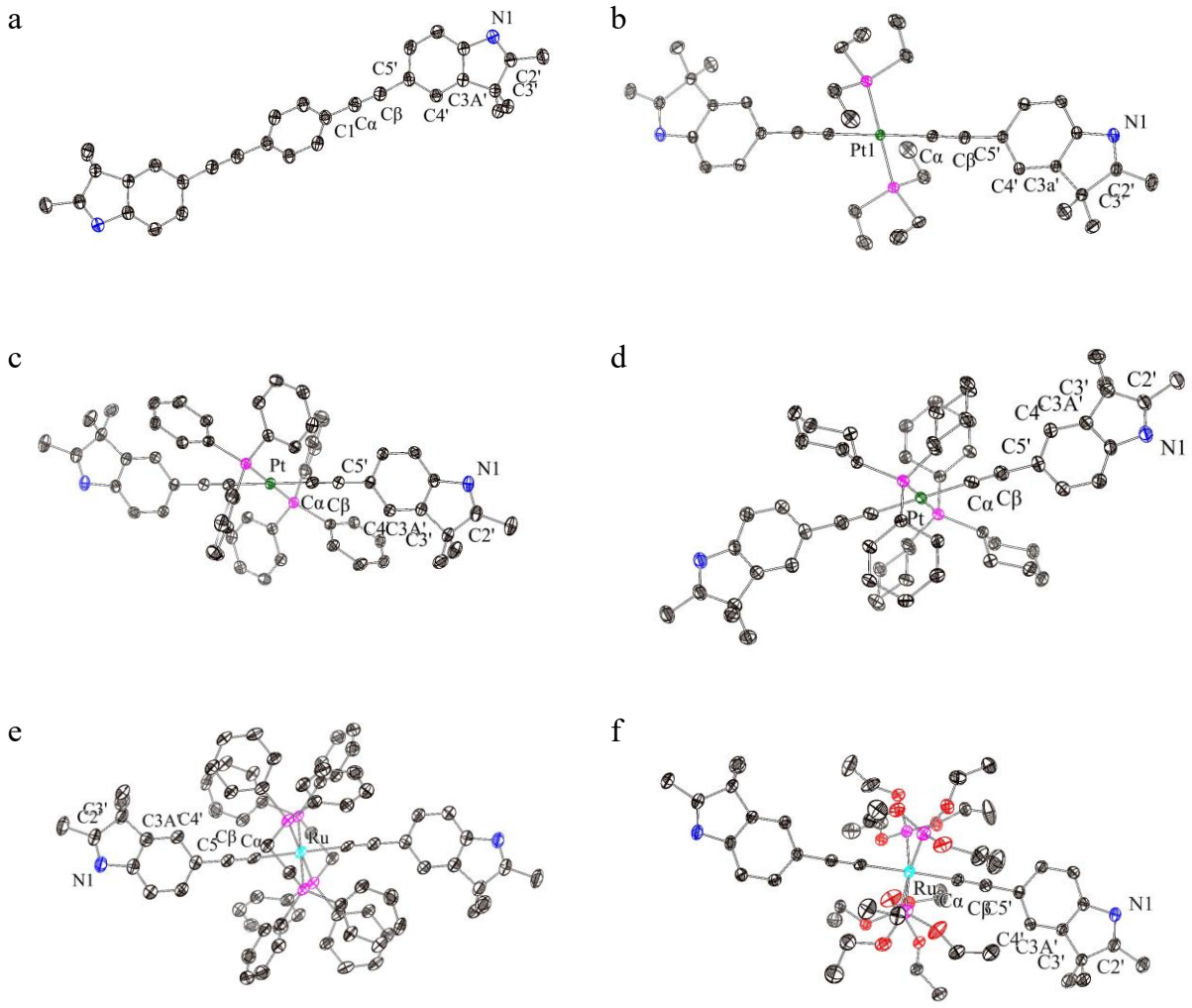

Figure 6. ORTEP representation of (a) **11**, (b) **12**, (c) **13**, (d) **15**, (e) **17** and (f) **18**, and atom numbering scheme. Ellipsoids drawn at 50% probability. Hydrogens and solvate omitted for clarity where appropriate.

Complex **18** shows the rod-like structure and pseudo-octahedral metal environment consistent with tetrakis(triethylphosphite) complexes (Figure 6). Moreover, the bond distances and angles are in the range previously described for these complexes.[61] Interestingly, the angle between planes of the aryl-ethynyl rings shows only a slight deviation from a coplanar orientation. Most complexes of this type adopt a twisted conformation between the aromatic groups.[60, 61] The M-P bond lengths are shorter in **18** than in **17** as a result of Ru-P π back-bonding.

Table 2. Selected bond lengths (Å) and bond and torsion angles (°) from the crystallographically determined structures

	Bond lengths (Å) and bond and torsion angles (°)													
	M-P	M-Cα	Cα-Cβ	Cβ-C5′	N1-C2′	P-M-P (*cis*)	P-M-P (*trans*)	Cα-M-Cα	M-Cα Cβ	Cα Cβ-C5′	C7A′-N1-C2′	θ	θ′	θ″
11		1.428(3)	1.209(3)	1.437(3)	1.301(3)				178.3(3)	176.2(3)	106.3(2)		35.0(3)	180.0(2)
12	2.2934(3)	1.9987(12)	2.2185(17)	1.4355(17)	1.2917(19)		180.0	180.0	178.81(12)	176.49(14)	106.51(11)		53.1	180.0(1)
13	2.3193(7)	1.994(3	1.218(5)	1.441(4)	1.287(5)		180.0(3)	180.0	178.9(3)	177.9(3)	106.5(3)		50.0	180.0(3)
15	2.3138(5)	2.003(2)	1.214(3)	1.443(3)			178.708(17)	177.51(8)	172.92(19)	174.7(2)			61.7(2)	39.4(3)
	2.3232(5)								178.02(19)	172.6(2)			58.8(2)	
16	2.3175(7)	2.034(3)	1.170(4)	1.440(4)	1.298(4)		180.0	180.0	176.9(2)	177.0(3)	106.6(3)		84.9	180.0(3)
17	2.3539(12)	2.092(5)	1.186(7)	1.434(7)	1.282(8)	82.37(4)	180.00(6)	180.0	176.0(4)	175.8(5)	106.3(5)	77.2		180.0(5)
	2.3592(12)													
18	2.3107(7)	2.075(3)	1.207(3)	1.440(3)	1.281(4)	89.27(3)	174.33(2)	178.04(10)	178.4(2)	178.4(2)	106.6(2)		44.4(2)	175.2(2)
	2.3114(7)	2.067(2)	1.207(3)	1.438(3)	1.284(4)	90.98(2)	173.31(3)		178.7(2)	177.4(3)	106.2(2)		41.2(2)	
	2.3202(7)					90.47(3)								
	2.3177(7)					89.95(3)								

θ is the torsion angle between the plane bisecting the dppe ligands and the plane of the arylethynyl ligand. θ′ is the lowest torsion angle between the C4′C5′-Ru-P (any). θ″ is the angle between the planes of the indole rings.

Bonds around the metal centres show slight variations. M-P bond lengths are longer in **17** than the Pt complexes, comparable to the bond lengths in **18**. There are slight geometric differences about the respective metal centres however these are less remarkable moving away from the metal. Bond lengths and angles in the indole rings show no significant differences between the metal complexes. All indole rings of the aryl-ethynyl complexes lie in the same plane allowing for delocalisation along the metal-alkyne backbone.

Electrochemistry

The electrochemical properties of the indole complexes were studied to compare the redox potentials as a function of the metal-ligand fragment (Table 3). The cyclic voltammograms of all complexes show single reversible oxidations at potentials between -640 mV and -60 mV (vs Fc/Fc^{+}) (E^{1}_{ox}) and additional irreversible oxidations between 580 and 780 mV (vs Fc/Fc+) (E^{2}_{ox}). The oxidation potentials are consistent with the indoline moiety being electron-donating.[39] The Cp* ligand moves the oxidation potential 200 to 300 mV more cathodic in both systems. The iron complexes undergo the first oxidation at potentials 300 to 400 mV more cathodic than their isostructural ruthenium complex. The second oxidation, presumably at the nitrogen of the indoline, is more dependent on the metal in the ruthenium complexes than in the iron complexes. This behaviour is predictable given the larger degree of delocalisation of electron density over the ruthenium acetylide.

Table 3. Electrochemical data for complexes **4** to **7**, and **17**.

	$E_{1/2}$ (E^{1}_{ox}) (V)	ΔE_p (E^{2}_{ox}) (V)	i_{pc}/i_{pa} (E^{1}_{ox})	E_{pa} (V) (E^{2}_{ox})
4	-0.06	0.09	0.92	0.74
5	-0.30	0.10	0.93	0.58

6	-0.64	0.10	1.03	0.77
7	-0.44	0.09	0.97	0.77
17	-0.12	0.09	1.01	0.71

All experiments are in CH_2Cl_2 solutions containing 0.1 M Bu_4NPF_6 supporting electrolyte using a Pt working electrode and Pt/Ti counter and pseudo-reference electrode. The decamethylferrocene/decamethylferricenium ($Fe(Cp^*)_2/[Fe(Cp^*)_2]^+$) couple was used as an internal reference, with all potentials reported relative to the ferrocene/ferricenium couple ($FeCp_2/[FeCp_2]^+$ = 0 V, such that $Fe(Cp^*)_2/[Fe(Cp^*)_2]^+$ = -0.55 V). Scan rate of 100 mV s^{-1} at room temperature. No correction for IR compensation was used.

Single-molecule conductance studies

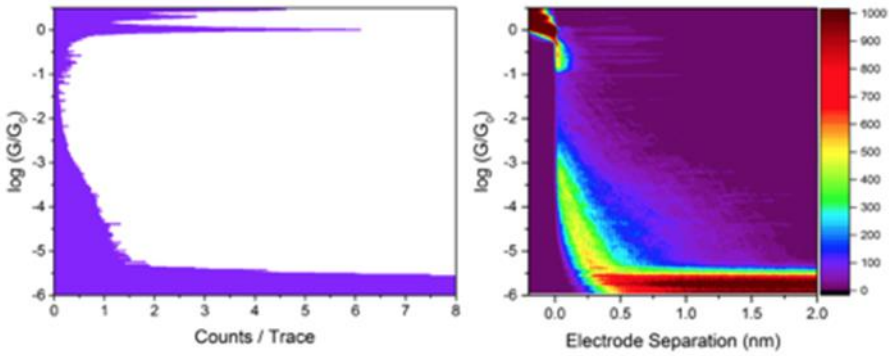

Figure 7. Normalised 1D conductance histogram and 2D conductance-displacement density plot for **11** using STM-BJ at 100 mV bias. More than 3000 individual breaking traces were compiled with no data selection.

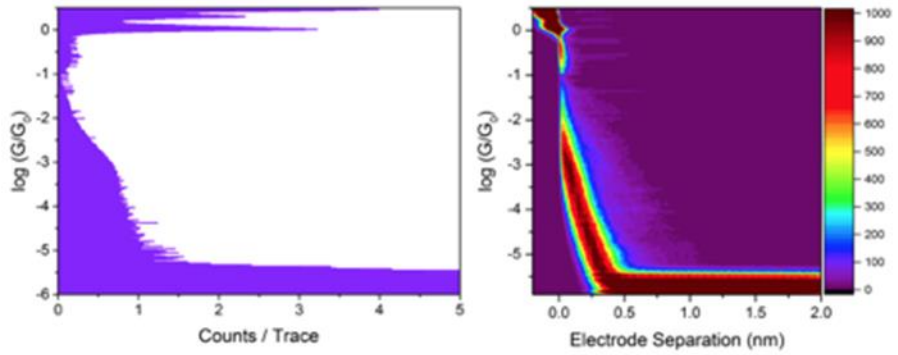

Figure 8. Normalised 1D conductance histogram and 2D conductance-displacement density plot for **12** using STM-BJ at 100 mV bias. More than 3000 individual breaking traces were compiled with no data selection.

Normalised conductance histograms (on the left) and density plots (on the right) are shown in Figure 7 and Figure 8 for compounds **11** and **12**, respectively. The conductance histograms show clear G_0 peaks at $\log(G/G_0) = 0$, which correspond to the single channel Au-Au metal atom point contact. The 2D density plots display log(conductance) versus electrode separation during the STM tip retraction from the metal point contact to 2.0 nm extension. As seen from these plots, there is little evidence of extended molecular junction formation and hence it is not possible to attribute a conductance peak to these compounds. Possible reasons for the absence of an apparent junction formation for these compounds could be a low junction formation probability or conductance values falling below the noise floor of about $10^{-5.5}$ G_0 ($G_0 = 2e^2/h = 77.5$ μS). A low junction probability could result from steric hindrance from the vicinal methyl group to the proposed nitrogen dative binding site of the specific indole terminal groups employed here. Low binding strength of amine contacting groups has been attributed to the steric influence of hydrogens.[89] However, if a junction is forming, then the conductance itself could be lower than the noise floor ($10^{-5.5}$ G_0), which would mean that it would lie out of the measurement window of the conductance determination. The molecular backbone is chemically similar to previous studied compounds (and their conductance): *trans*-Pt(CC-CC_6H_4-CC-$SiMe_3$)$_2$(PEt_3)$_2$ ($3.2 \pm 1.3 \times 10^{-5}$ G_0),[56] *trans*-Pt(CC-cyclo-3-C_4H_3S)$_2$(PEt_3)$_2$ ($2.70 \pm 0.66 \times 10^{-4}$ G_0), and 1,4-C_6H_4(CC-cyclo-3-C_4H_3S)$_2$ ($2.83 \pm 0.65 \times 10^{-4}$ G_0),[90] all of which displayed molecular conductance values greater than 10^{-5} G_0 (i.e. greater than the noise floor of our present measurements). Additionally, OPEs with a similar backbone structure to compound **12** show conductance values of $2.6 \pm 1.6 \times 10^{-5}$ to

$3.6 \pm 1.6 \times 10^{-5}$ G_0.[91] Therefore, it seems rational to assume the primary cause for no apparent molecular junction formation is inherent to the new contact group. This lack of junction formation may be related to insufficient dative bonding between the N of the indole terminal groups and the gold electrodes or may arise from steric hindrance of this bonding as a result of the vicinal methyl group.

Steric hindrance can impede potential anchoring groups binding to gold contacts, for example, previous studies have noted that the high conductance hollow geometric formation seen in bipyridyl ethyne is inhibited by introducing vicinal C-F bonds.[92] It is instructive to consider how junctions might form in the STM-BJ experiment for compounds **11** and **12**. Analogous pyridyl anchoring groups (e.g. in 4,4′ bipyridine molecular bridges with gold contacts[93]) evolve from a face-on alignment of the pyridyl ring to an end on dative binding of the terminal N atom to a Au apex atom. As an anchor group slides across the pyramidal tip through a side configuration, it can jump to an apex position to form the final molecular junction.[94] If a similar mechanism is assumed here for our indole contact group, this last jump could be impeded by the vicinal methyl group, leading to a complete rupture. Another possible issue might be the chemical stability of the molecules under the experimental conditions needed to form Au-molecule-Au junctions. An pyrrolic-type indole terminated diarytetrayne has been shown not to exhibit junction formation due to the chemical and thermal instability of the moiety under the employed experimental conditions.[95] However, given the ambient stability of the compounds synthesised in this study, we believe that that degradation during single-molecule conductance experiments is less likely to cause absence of junction formation features. The last reason we postulate for the absence of junctions for compounds **11** and **12** is the slight increase in basicity of the indole contact group (pKa of the conjugated acid 6.33) compared to the pyridine contact group (pKa of the conjugated

acid 5.25). Hard-soft acid-base (HSAB) theory has been shown to predict the formation of metal-molecule junctions with lone pairs on the anchoring group (e.g. pyridyl, amine) and gold electrodes.[96] While pyridine is of an "intermediate" character on the hard-soft continuum, it seems possible that the increase in basicity of the 3*H*-indole reduces its affinity for the gold electrodes if there is a less favourable HSAB match.

Spectroelectrochemistry

Spectroelectrochemical methods have become useful tools to determine the nature of redox processes and redox products for metal alkynyl complexes.[97] The complexes **4**, **7** and **17** were chosen for spectroelectrochemical investigations to act as models across the series of compounds in this study and due to the ease of comparison to other similar species studied in the literature.

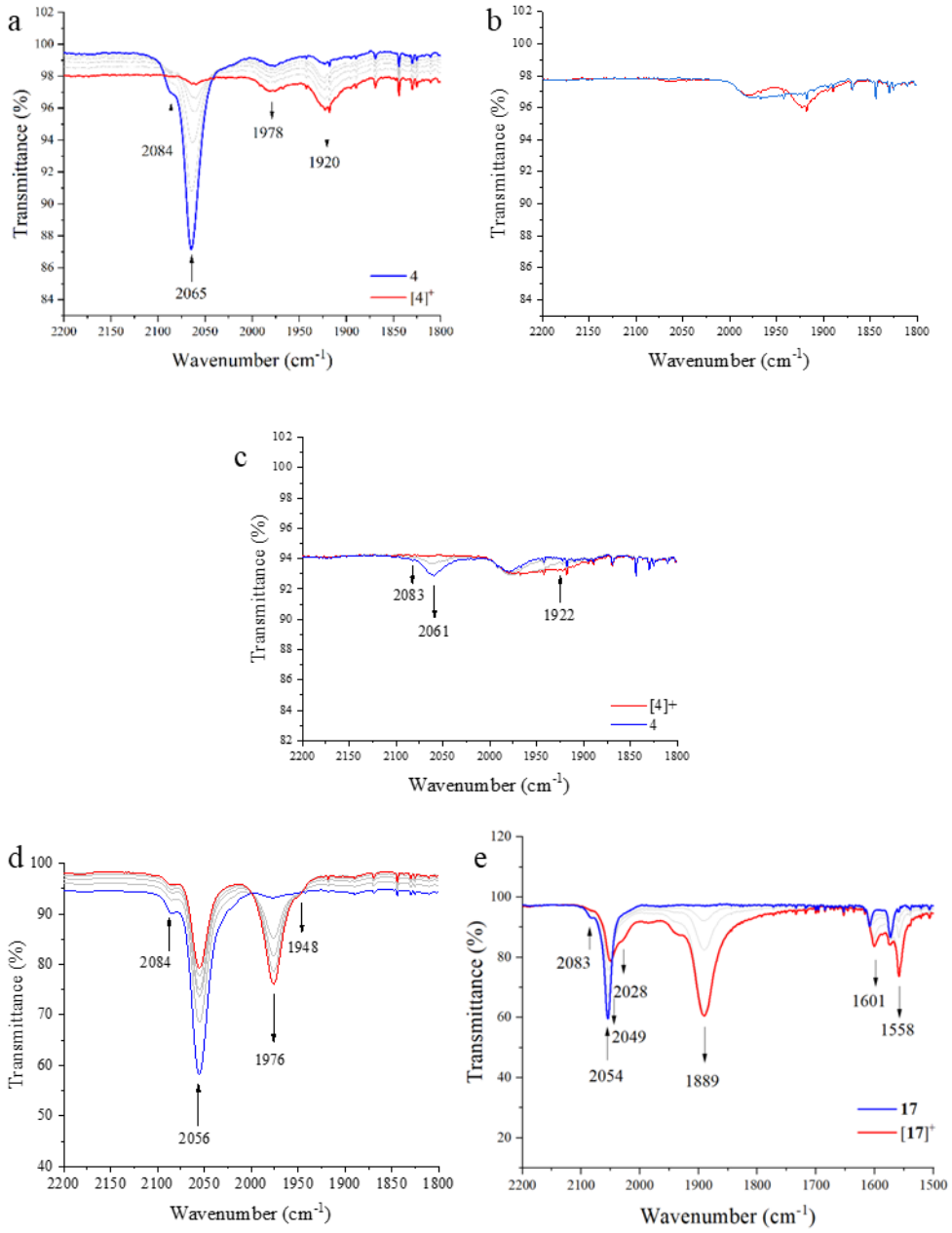

Figure 9. IR spectra of complexes (a, b and c) $[\mathbf{4}]^{n+}$ (n = 0, 1), (d) $[\mathbf{7}]^{n+}$ (n = 0, 1) and (e) $[\mathbf{17}]^{n+}$ (n = 0, 1) recorded in a spectroelectrochemical cell (CH_2Cl_2/0.1M Bu_4NPF_6)

The infrared spectroelectrochemical spectra of complexes **4** and **7** during the first oxidation are illustrated in Figure 9 and 10, respectively. The IR spectra of the neutral complex **4** shows a single absorption at 2065 cm^{-1} assigned to the ν(Ru-C≡C) band. Upon oxidation the band decreases in

intensity. A small IR absorption for the ν(Ru-C≡C) band was observed for the oxidized complex [**4**]$^+$ at 1920 cm^{-1}.[39] Complex [**4**]$^+$ was unstable on the timescale of spectroelectrochemical experiments with the decay of the band assigned to the ν(Ru-C≡C) at 1920 cm^{-1} over a short period of time. However, we can confidently assign this band to the ν(Ru-C≡C) as reduction exchanges this band for the ca. 2060 cm^{-1} for complex **4**. We note also the possible formation of the [Ru(Cp)(PPh$_3$)$_2$(CO)]$^+$ cation upon the appearance of the band at ca. 1970 cm^{-1}. For the iron complex **7**, two active ν(Fe-CC) modes were observed upon oxidation. A shift of Δ80 cm^{-1} in the ν(Fe-CC) absorption band is in agreement with iron complexes of the type Fe(CCR)(dppe)Cp, and is consistent with a large degree of metal character in the first oxidation process.[39] The appearance of two broad active ν(Fe-C≡C) modes can be rationalized as a population of local states on the potential energy surface, where several accessible conformers that differ by the orientation the arylethynyl ligand with respect to the metal orbitals.[98]

The IR spectra upon oxidation of **17** to [**17**]$^+$ is illustrated in Figure 10. The complex **17** is characterised by an absorption at 2054 cm^{-1} assigned to the ν(Ru-C≡C) stretch. Upon oxidation to the monocations, [**17**]$^+$, the ν(Ru-C≡C) assigned absorption band shifts by 165 cm^{-1} to 1889 cm^{-1}. This large shift is indicative of the large contribution of the alkynyl ligand to the oxidation process. The broad and asymmetric nature of the ν(Ru-C≡C) envelope in [**17**]$^+$ is consistent with a range of conformer which vary as a result of the relative orientation the arylethynyl ligands with respect to the metal centre.[63] A weak feature between 2049 and 2028 cm^{-1}, is consistent with additional conformers with electronic structures localized over one arylethynyl ligand.[60] The additional absorption at 1601 and 1558 cm^{-1} is likely assigned to aryl breathing modes, further consistent with the large contribution of the ethynyl ligand in the oxidation process.

Conclusion

The synthesis of new 3*H*-indole functionalized σ-alkynyl complexes has been achieved. These new ligands protonate at the imine nitrogen atom and can form multicomplex architectures with copper. The complexes show reversible electrochemical behaviour that is localized over the metal-alkynyl component. The results suggest a broad scope of future work can be explored for these ligands in polymetallic complexes and frameworks and moderation of opto-electrical properties from such complexes.

Experimental

General

All reactions were carried out under high purity argon or nitrogen using Schlenk techniques and oven-dried glassware. All solvents for reactions were dried by distillation under argon over an appropriate drying agent or by an Innovative technologies SPS and deoxygenated (freeze/pump/thaw or sparging) before use. Hexanes and EtOAc for column chromatography were distilled before use. All other solvents were of AR grade and used without further purification. Unless otherwise stated, no special precautions were taken to exclude air or moisture during work-up and purification. All other reagents were used as received from their supplier. Flash column chromatography was carried out using silica gel 60 (0.04 – 0.063) or alumina (Brockmann activity IV, basic). Thin layer chromatography was carried out using Merck silica gel 60 F254 pre-coated aluminium sheets.

Instruments

^{1}H, ^{13}C{^{1}H}, ^{31}P{^{1}H}, and ^{19}F NMR spectra were recorded at 25°C on a Bruker 600 MHz, 500 MHz, or 400 MHz spectrometer. Chemical shifts (δ) are referenced to the internal undeuterated residual solvent signal (1H), deuterated solvent signal (13C) or external standard (^{31}P, 85%

H_3PO_4). First order multiplets are as follows: s (singlet), d (doublet), t (triplet), q (quartet), quin (quintet), sext (sextet), oct (octet), dd (doublet of doublets), ddd (doublet of doublet of doublets), dt (doublet of triplets), tt (triplet of triplets). Apparent multipets are labelled with the prefix 'app.'. Broad signals are labelled with the prefix 'br.'. Multiplets of higher order or undeterminable are labelled as multiplet (m). Coupling constants (J) are reported in hertz (Hz). Signal assignments were made with help from HSQC, HMBC and COSY experiments, spectrum prediction software and literature precedent. Infrared spectroscopy was carried out as neat products using an ATR module fitted FTIR spectrometer. Electrospray ionisation (ESI) or atmospheric-pressure chemical ionisation (APCI) mass spectrometry was carried out on a Waters LCT Premier TOF spectrometer. Electron impact ionisation was carried out using a Waters GCT Premier or Shimadzu GCMS QP2010. In most cases, HPLC grade acetonitrile was used as the solvent. If needed, a couple of drops of dichloromethane was used to help solubilise the compound for analysis. Melting points were collected on a Buchi M-565. Elemental analyses were performed by Stephen Boyer, London Metropolitan University, London, United Kingdom.

Synthesis

The compounds **1**, $[RuCl(dppe)_2]OTf$,[44] $Ru(dppe)(Cp^*)Cl$,[99] $CpRu(PPh_3)_2(Cp)Cl$,[100] $Fe(dppe)(Cp^*)Cl$,[99] $Fe(dppe)(Cp)Cl$,[99] PPh_3AuCl[101] and $Ru(CO)_2(Cp)Cl$[102] were synthesised according to literature procedures.

5-ethynyl-2,3,3-trimethyl -3*H*-indole (2)

A round bottom charged with 2,3,3-trimethyl-5-trimethysilylalkynyl-3H-indole (3.01 g, 0.012 mol) (**1**) was dissolved in THF (20 mL). This solution was sparge deoxygenated with argon for 20 min. Simultaneously, KOH (750 mg, 0.013 mol) was dissolved in MeOH (20 mL) and sparged with argon. The THF solution was cannula transferred into the methanolic solution with stirring.

The solution was stirred for 3 hours. The solvent was taken to dryness under reduced pressure. The residue of dissolved in Et_2O (50 mL) and washed with water (3 x 50 mL). Additionally, the aqueous solution was back extracted with Et_2O (50 mL). The combined organic phases were washed with brine (1 x 50 mL), dried over $MgSO_4$, and evaporated to dryness. The yellow oily residue was subject to chromatography (silica; 30% EtOAc/hexanes) to give yellow oil that solidifies upon standing (1.90 g, 86%). Crystals for XRD were grown by slow evaporation of a Et_2O solution. mp: 50 – 51 °C. ^{1}H NMR ($CDCl_3$, 500 MHz): δ 7.40 – 7.47 (m, 3H), 3.07 (s, 1H, CC-H), 2.28 (s, 3H, C2-CH_3), 1.29 (s, 6H, *gem*-CH_3). $^{13}C\{^1H\}$ NMR ($CDCl_3$, 125 MHz): δ 189.7 (s, C2), 154.3 (s, C7a), 145.9 (s, C3a), 132.3 (s, C6), 125.3 (s, C4), 120.0 (s, C7), 118.7 (s, C5), 84.3 (s, Cβ), 77.0 (s, Cα), 53.9 (s, C3), 23.1 (s, C2-CH_3), 15.6 (s, *gem*-CH_3). IR (ATR, neat) ν_{max} / cm^{-1}: 3176 (C-H), 2958, 2972, 2926, 2099 (C≡C), 1571 (C=N), 1458. HRMS (APCI(+), MeCN) *m/z*: calcd for $C_{13}H_{14}N^+$ 184.1121 $[M+H]^+$, found 184.1118. Anal. Calcd for $C_{13}H_{13}N$: C, 85.21; H, 7.15; N, 7.64. Found: C 85.15; H, 7.03; N 7.57.

(*E*)-1,2-bis(5-ethynyl-3,3-dimethyl-3H-indol-2-yl)-ethene (3)

Isolated as a yellow powder. Crystals grown by slow evaporation of a Et_2O solution. ^{1}H NMR ($CDCl_3$, 600 MHz): δ 7.61 – 7.63 (m, 4H, H4 & H7), 7.52 (dd, *J* = 1.2, 7.8 Hz, 2H, H6), 7.46 (br, s, 2H, H8), 3.15 (s, 2H, C≡C-H), 1.48 (s, 12H, *gem*-CH_3). $^{13}C\{^1H\}$ NMR ($CDCl_3$, 126 MHz): δ 183.8 (s, C2), 154.2 (C7a), 147.1 (C3a), 132.7 (C6), 128.5 (C8), 125.3 (C4), 121.4 (C7), 120.3 (C5), 84.1 (Cβ), 78.0 (Cα), 53.2 (C3), 23.3 (*gem*-CH_3). IR (ATR, neat) ν_{max} / cm^{-1}: 3302 (H-C≡), 3243 (H-C≡), 2104 (C≡C), 1607 (C=C), 1508 (C=N), 1454. HRMS (APCI(+), MeCN) *m/z*: calcd for $C_{26}H_{23}N_2^+$ 363.1856 $[M+H]^+$, found 363.1851.

Ru(PPh_3)$_2$(Cp)(ethynyl-2,3,3-trimethyl-3*H*-Indole) (4)

A solution of $Ru(PPh_3)_2(Cp)Cl$ (199 mg, 0.274 mmol), **2** (100 mg, 0.546 mmol) and NH_4PF_6 (219 mg, 1.34 mmol) were refluxed in MeOH (20 mL) for 1 hour to give a dark red solution. The solution was cooled to ambient temperature and stirring ceased. A slight excess of DBU (0.15 mL) was slowly added dropwise and the solution was left undisturbed overnight and then cooled in an ice bath. The yellow crystals were collected by filtration and washed with cold MeOH and cold Et_2O, dried in air, and then dried under vacuum (165 mg, 69%). Crystals for XRD were grown by diffusion on pentane in a concentrated CH_2Cl_2 solution. ^{1}H NMR ($C6D_6$, 400 MHz): δ 7.80 (d, J 8.0 Hz, 1H, H7), 7.73 – 7.78 (m 12H, Hmeta), 7.60 (dd, J = 1.6, 7.9 Hz, 1H, H6), 7.42 (d, J = 1.5 Hz, 1H, H4), 6.92 – 6.99 (m, 18H, Hpara and Hortho), 4.51 (s, 5H, Cp), 2.00 (s, 3H, $NCCH_3$), 1.01 (s, 6H, *gem*-CH_3). $^{13}C\{^1H\}$ NMR (C_6D_2, 100 MHz): δ 184.6 (C2), 151.5 (C7a), 146.0 (C3a), 139.3 (m, Cipso), 134.4 (t, *J* = 5 Hz, Cmeta), 130.4 (C6), 128.7 (Cpara), 128.1 (C5), 127.6 (t, *J* = 5 Hz, Cortho), 124.3 (C4), 120.2 (C7), 116.1 (Cβ), 113.8 (t, *J* = 26 Hz, Cα) 85.7 (Cp), 53.2 (C3), 23.2 (*gem*-CH_3), 15.1 (NCCH3). $^{31}P\{^1H\}$ NMR (CD_2Cl_2, 202 MHz): δ 50.6 (s, dppe). IR (ATR, neat) ν_{max} / cm^{-1}: 2060 (C≡C). HRMS (ES(+), MeCN) *m/z*: calcd for $C_{54}H_{49}NP_2Ru^{2+}$ $[M+2H]^{2+}$ 437.6187, found 437.6174, calcd for $C_{43}H_{38}NP_2Ru^+$ $[M-L+MeCN]^+$ 732.1518, found 732.1575, calcd for $C_{54}H_{48}NP_2Ru^+$ $[M+H]^+$ 874.2300, found 874.2360.

Ru(dppe)(Cp*)(ethynyl-2,3,3-trimethyl-3*H*-Indole) (5)

A solution of Ru(dppe)(Cp*)Cl (103 mg, 0.154 mmol), **2** (89 mg, 0.486 mmol) and NH_4PF_6 (150 mg, 0.920 mmol) were refluxed in MeOH (10 mL) for 3 hours to give a dark red solution. The solution was cooled to room temperature and stirring was ceased. An excess of DBU (0.15 mL) was slowly added dropwise and the solution was left undisturbed overnight and then cooled in an ice bath. The yellow needles were collected by filtration and washed with cold MeOH and cold pentane, dried in air, and then dried under high vacuum (101 mg, 80%). Crystals for XRD were

grown by cooling a Et_2O/pentane solution. ^1H NMR (C_6D_6, 600 MHz): δ 7.92 – 7.95 (m, 4H, Hpara), 7.67 (d, J = 7.8 Hz, 1H, H7), 7.07 – 7.28 (m, 17H, Hortho & Hmeta & H6), 6.95 (d, J = 2 Hz, 1H, H4), 2.60 – 2.70 (m, 2H, dppe-CH_2), 1.96 (s, 3H, $NCCH_3$), 1.84 – 1.88 (m, 2H, dppe-CH_2), 1.68 (s, 15H, Cp*), 0.96 (s, 6H, *gem*-CH_3). $^{13}C\{^1H\}$ NMR (C_6D_6, 100 MHz): δ 184.3 (C2), 151.2 (C7a), 145.8 (C3a), 139.8 (m, Cipso), 137.8, 137.5, 134.3 (t, J = 5 Hz, Cortho), 133.7 (t, J = 5 Hz, Cortho), 130.3 (C6), 129.2 (PPh_2) 129.0 (PPh_2), 128.8 (PPh_2), 128.7 (PPh_2), 128.2 (PPh_2), 128.0 (PPh_2), 127.7 (PPh_2) 127.6 (PPh_2), 127.4 (PPh_2), 127.1 (t, J = 25 Hz, Cα) 123.8 (C4), 120.0 (C7), 111.4 (Cβ), 92.8 (t, J = 2 Hz, Cp), 53.1 (C3), 29.9 (m, dppe-CH_2), 23.2 ($NCCH_3$), 15.1 (s, *gem*-CH_3), 10.4 (s, $Cp(CH_3)_5$). $^{31}P\{^1H\}$ NMR (C_6D_6, 243 MHz): δ 81.6 (s, dppe). IR (ATR, neat) ν_{max} / cm^{-1}: 2058 (C≡C). HRMS (ES(+), MeCN) *m/z*: calcd for $C_{49}H_{53}NP_2Ru^{2+}$ $[M+2H]^{2+}$ 409.6343, found 409.6335, calcd for $C_{37}H_{39}OP_2Ru^+$ $[M-L+CO]^+$ 663.1515, found 663.1531, calcd for $C_{38}H_{42}NP_2Ru^+$ $[M-L+MeCN]^+$ 676.1831, found 676.1961, calcd for $C_{49}H_{52}NP_2Ru^+$ $[M+H]^+$ 818.2613, found 818.2619.

Fe(dppe)(Cp*)(ethynyl-2,3,3-trimethyl-3*H*-Indole) (6)

A yellow solution of Fe(dppe)(Cp*)Cl (193 mg, 0.309 mmol), **2** (81 mg, 0.44 mmol) and NH_4PF_6 (100 mg, 0.613 mmol) were refluxed in MeOH (20 mL) for 2 hours to give a dark solution. The solution was cooled to room temperature and stirring was stopped. DBU (0.15 mL, excess) was slowly added dropwise and the solution was left undisturbed overnight and then cooled in an ice bath. The dark red needles were collected by filtration and washed with cold MeOH and cold pentane, dried in air, and then dried under vacuum (202 mg, 85%). Crystals for XRD were grown by diffusion of pentane in a concentrated CH_2Cl_2 solution. ^1H NMR (C_6D_6, 600 MHz): δ 8.04 – 8.07 (m, 4H, Hpara), 7.70 (d, J = 7.9 Hz, 1H, H6), 7.01 – 7.34 (m, 18H, H7 & H4 & Hortho & Hmeta), 2.61 – 2.70 (m, 2H, dppe-CH_2), 1.97 (s, 3H, $NCCH_3$), 1.81 – 1.87 (m, 2H, dppe-CH_2),

1.56 (s, 15H, Cp*), 0.97 (s, 6H, *gem*-CH_3). $^{13}C\{^1H\}$ NMR (C_6D_6, 151 MHz): δ 184.4 (C2), 151.1 (C7a), 146.0 (C3a), 139.8 (PPh_2), 138.3 (C5), 138.0 (PPh_2), 134.8 (PPh_2), 134.4 (PPh_2), 130.1 (C6), 129.2 (PPh_2), 129.0 (PPh_2), 128.3 (PPh_2), 128.1 (PPh_2), 128.0 (PPh_2), 127.5 (PPh_2), 123.5 (C4), 121.1 (^1H-$^{13}C\{^1H\}$ HMBC, Cβ), 120.2 (C7), 87.8 ($Cp(CH_3)_5$), 53.2 (C3), 31.2 (m, dppe-CH_2), 23.3 (s, $NCCH_3$) 15.1 (*gem*-CH_3), 10.48 ($Cp(CH_3)_5$), (Cα) not observed. $^{31}P\{^1H\}$ NMR (C_6D_6, 243 MHz): δ 100.87 (s, dppe). IR (ATR, neat) ν_{max} / cm^{-1}: 2045 (C≡C). HRMS (ES(+), MeCN) *m/z*: calcd for $C_{49}H_{52}FeNP_2^{2+}$ $[M+H]^{2+}$, found 386.142, calcd for $C_{49}H_{51}FeNP^+$ $[M]^+$ 771.2835, found 771.2824 $[M]^+$.

Fe(dppe)(Cp)(ethynyl-2,3,3-trimethyl-3*H*-Indole) (7)

A yellow solution of Fe(dppe)(Cp)Cl (196 mg, 0.353 mmol), **2** (86 mg, 0.47 mmol) and NH_4PF_6 (91 mg, 0.56 mmol) were refluxed in MeOH (15 mL) for 2 hours to give a dark brown solution. The solution was cooled to room temperature and stirring was finished. A slight excess of DBU (0.15 mL) was slowly added dropwise and the solution was left undisturbed overnight and then cooled in an ice bath. The dark red needles were collected by filtration and washed with cold MeOH and cold pentane, dried in air, and then dried under vacuum (179 mg, 72%). Crystals for XRD were grown by diffusion off pentane into a concentrated CH_2Cl_2 solution. ^1H NMR (C_6D_6, 600 MHz): δ 8.02 (br. s, 4H, Hpara), 7.55 (d, J = 7.9 Hz, 1H, H7), 7.20 – 7.27 (m, 10H, Hortho & meta), 6.98 – 7.04 (m, 6H, Hortho & Hmeta), 6.92 (d, J = 7.9 Hz, 1H, H6), 6.70 (s, 1H, H4), 4.32 (s, 5H, Cp), 2.49 – 2.58 (m, 2H, dppe-CH_2), 1.90 – 1.98 (m, 5H, $NCCH_3$ & dppe-CH_2), 0.92 (s, 6H, *gem*-CH_3). $^{13}C\{^1H\}$ NMR (C_6D_6, 100 MHz): δ 184.4 (C2), 151.2 (C7a), 145.6 (C3a), 143.0 (m, PPh_2), 138.9 (m, PPh_2), 134.2 (t, PPh_2), 132.2 (t, PPh_2), 129.9 (C6), 129.3 (PPh_2), 128.8 (PPh_2), 128.7 (PPh_2), 128.3 (PPh_2), 128.2 (PPh_2), 128.0 (PPh_2), 124.1 (C4), 122.7 (Cβ), 122.3 (t, J = 42 Hz, Cα), , 119.8 (C7), 79.5 (Cp), 53.0 (C3), 28.7 (m, dppe-CH_2), 23.2 (s, $NCCH_3$), 15.1 (s, *gem*-

CH_3), C5 obscured. $^{31}P\{^1H\}$ NMR (C_6D_6, 243 MHz): δ 106.94 (s, dppe). IR (ATR, neat) ν_{max} / cm^{-1}: 2055 (C≡C). HRMS (ES(+), MeCN) *m/z*: calcd for $C_{44}H_{42}FeNP_2^{2+}$ $[M+H]^{2+}$ 351.1063, found 351.1048, calc for $C_{46}H_{45}FeN_2P_2^{2+}$ $[M+H+MeCN]^{2+}$ 371.6196, 371.6192, calcd for $C_{33}H_{32}FeNP_2^{+}$ $[M-L+MeCN]^{+}$ 560.1349, found 560.1346, calcd for $C_{44}H_{41}FeNP^{2+}$ $[M]^{+}$ 701.2053, found 701.2095 $[M]^{+}$.

$Ru(CO)_2$(Cp)(ethynyl-2,3,3-trimethyl-3*H*-Indole) (8)

$Ru(CO)_2(Cp)Cl$ (102 mg, 0.393 mmol), **2** (79 mg, 0.431 mmol), CuI (5 mg) were charged to a Schlenk flask and the solids were suspended in NEt_3 (10 mL) and THF (10 mL). The light yellow solution was stirred for 24 hours covered in foil. The solution was then evaporated in vacuo, and the residue was extracted with Et_2O and filtered through cotton wool until the washings were colourless. The Et_2O was removed by rotary evaporation and the orange residue was columned on basic alumina using CH_2Cl_2 / CH_3OH (99 / 1). The yellow band was collected and the solvent removed to give a yellow powder (111 mg, 70%). Crystals for XRD were obtained by slow cooling of a Et_2O/pentane solution to yield yellow plates. ^1H NMR ($CDCl_3$, 600 MHz): δ 7.35 (d, *J* = 7.8Hz, 1H, H7), 7.28 – 7.29 (m, 2H, H4 & H6), 5.48 (s, 5H, Cp), 2.24 (s, 3H, $NCCH_3$), 1.26 (s, 6H, *gem*-CH_3). $^{13}C\{^1H\}$ NMR ($CDCl_3$, 151 MHz): δ 196.9 (CO), 187.7 (C2), 151.6 (C7a), 145.4 (C3a), 131.3 (C6), 124.9 (C7), 124.2 (C5), 119.4 (C4), 111.0 (Cβ), 88.1 (Cp), 81.3 (Cα), 53.6 (C3), 23.3 ($NCCH_3$), 15.51 (s, *gem*-CH_3). IR (ATR, neat) ν_{max} / cm^{-1}: 2119 (C≡C), 2035 (C≡O), and 1994 (C≡O). HRMS (ES(+), MeCN) *m/z*: calcd for $C_{20}H_{18}NO_2Ru^{+}$ $[M+H]^{+}$ 406.0376, found 406.0388. Anal Calcd for $C_{20}H_{24}NO_2Ru$: C, 59.40; H, 4.24; N, 3.46. Found: C 59.11; H, 4.57; N 3.52.

(PPh_3)Au(ethynyl-2,3,3-trimethyl-3*H*-Indole) (9)

An argon filled Schlenk flask was charge with (PPh_3)AuCl (49 mg, 0.099 mmol), **2** (23 mg, 0.12 mmol) and NaOMe (8 mg, 0.1 mmol) were stirred in MeOH (20 mL) in the dark for 3 hours. The reaction was concentrated and cooled in a freezer. The yellow powder formed was collected by filtration and washed with cold MeOH and Et_2O (27 mg, 42%). Crystals for XRD were grown by slow evaporation of a THF/EtOH/heptane solution to yield yellow plates. ^{1}H NMR (C_6D_6, 600 MHz): δ 7.86 (dd, *J* = 8.0, 1.3 Hz, 1H, H6), 7.72 (d, *J* = 1.3 Hz, 1H, H4), 7.61 (d, *J* = 8.0 Hz, 1H, H7), 7.25 – 7.29 (m, 3H, Hpara), 6.94 – 6.97 (m, 6H, Hmeta), 6.87 – 6.90 (m, 6H, Hortho), 1.88 (s, 3H, $NCCH_3$), 0.82 (s, 6H, *gem*-CH_3). $^{13}C\{^1H\}$ NMR (C_6D_6, 151 MHz): δ 186.6 (C2), 153.7 (C7a), 146.2 (C3a), 135.8 (d, *J* = 146 Hz, Cα), 134.5 (d, *J* = 14 Hz, Cortho), 132.6 (C6), 131.2 (d, *J* = 1.6 Hz, Cpara), 130.6 (d, *J* = 55 Hz, Cipso), 129.2 (d, *J* = 11 Hz, Cmeta), 125.8 (C4), 123.8 (C5), 120.4 (C7), 104.1 (d, *J* = 26 Hz, Cβ), 53.4 (C3), 22.8 (s, $NCCH_3$), 15.0 (s, *gem*-CH_3). $^{31}P\{^1H\}$ NMR (C_6D_6, 243 MHz): δ 42.2 (s, PPh_3). IR (ATR, neat) ν_{max} / cm^{-1}: 1574, 1480, 1456, 1434. HRMS (ES(+), MeCN) *m/z*: calcd for $C_{20}H_{18}AuNP^+$ $[M\text{-}L+MeCN]^+$ 500.0838, found 500.0844 $[M\text{-}L+MeCN]^+$, calcd for $C_{31}H_{28}AuNP^+$ $[M+H]^+$ 642.1620, found 642.1627, calcd for $C_{36}H_{30}AuP_{2+}$ $[Au(PPh_3)_2]^+$ 721.1483, found 721.1501, calcd for $C_{49}H_{42}Au_2NP_2^+$ $[M+(M\text{-}L)]^+$ 1100.2119, found 1100.2175.

Reaction of [Ru(dppe)$_2$Cl]OTf with 2 to give 10a/10b

A Schlenk tube charged with [Ru(dppe)$_2$Cl]OTf (99 mg, 0.0915 mmol) and **2** (18 mg, 0.098 mmol) was placed under high vacuum for 30 minutes and refilled with argon. CH_2Cl_2 (5 mL) was then added and the solution was stirred overnight. Evaporation of the solvent yielded a yellow-red residue that was washed with diethyl ether. The residue was dissolved in a minimum amount of dry dichloromethane and dry diethyl ether was then added to form a biphasic system and the vessel was placed in the freezer. A green-yellow solid was decanted away from the mother liquors and

washed with diethyl ether and pentane and dried under high vacuum (91 mg). Further recrystallization attempts could not eliminate side-products. ^{1}H NMR (CD_2Cl_2, 500 MHz): δ 6.91 – 7.47 (m, 41H), 6.70 (s 1H), 6.25 (s, 1H), 2.69 (br. app. s, 11H, dppe & NCH_3), 1.45 (s, 6H, *gem*-CH_3). ^{13}C{^{1}H} NMR (CD_2Cl_2, 126 MHz): δ 136.6, 135.0, 134.5, 134.4, 131.8, 129.6, 129.2, 128.5, 127.6, 127.5, 30.8, 23.3, 15.70. ^{31}P{^{1}H} NMR (CD_2Cl_2, 202 MHz): δ 48.3 (s, 10a), 41.7 (s, unknown), 37.3 (s, 10b) (unreferenced). ^{19}F{^{1}H} NMR (CD_2Cl_2, 470 MHz): δ -79.0 (s, OTf) (unreferenced). HRMS (ES(+), MeCN) *m/z*: calcd for $C_{67}H_{64}N_2P_4Ru^{2+}$ $[M\text{-}Cl+MeCN+H]^{2+}$ 561.1526, found 561.1526, calcd for $C_{69}H_{67}N_3P_4Ru^{2+}$ $[M\text{-}Cl+2MeCN+H]^{2+}$ 581.6659, found 581.6659, calcd for $C_{67}H_{63}N_2P_4Ru^{+}$ $[M\text{-}Cl+MeCN]^{+}$ 1121.2985, found 1121.3201.

1,4-(2,3,3-trimethyl-5-alkynyl-3H-indole)-benzene (11)

Into an oven dried and argon filled reflux apparatus was added anhydrous NEt_3 (20 mL) and sparged with argon for 1 hour. To the degassed NEt_3 was added 1,4-diiodobenzene (158 mg, 0.479 mmol), **2** (202 mg, 1.10 mmol), CuI (10 mg) and $PdCl_2(PPh_3)_2$ (18 mg). The lemon-yellow solution was heated to reflux and stirred overnight. After cooling to ambient temperature the solution was filtered and evaporated to dryness *in vacuo*. The orange residue was dissolved in EtOAc (40 mL) and washed with water (3 x 20 mL) and brine (20 mL). The organic layer was dried over $MgSO_4$, filtered and evaporated to dryness. Flash silica chromatography using 1:1 EtOAc/hexanes yielded a yellow-to-orange powder (201 mg, 95%). Crystals grown by diffusion of cyclohexane into a concentrated $CHCl_3$ solution. ^{1}H NMR ($CDCl_3$, 500 MHz): δ 7.46 – 7.50 (m, 5H, Ar), 2.30 (s, 3H, CH_3), 1.32 (s, 6H, *gem*-CH_3). ^{13}C{^{1}H} NMR ($CDCl_3$, 125 MHz): δ 189.6, 154.1, 146.0, 131.8, 131.6, 124.8, 123.2, 120.1, 119.7, 91.9, 89.1, 53.9, 23.4, 15.7. IR (ATR, neat) ν_{max} / cm^{-1}: 2964, 2203 (C≡C), 1736, 1568, 1510, 1461. HRMS (AP(+), MeCN) *m/z*: calcd for $C_{32}H_{29}N_2^{+}$ $[M+H]^{+}$ 441.2331, found 441.2338.

***trans*-[bis(triethylphosphine)-bis(5-ethynyl-2,3,3-trimethyl-3*H*-indole)platinum] (12)**

An oven dried and argon filled reflux apparatus was charged with $Pt(PEt_3)_2Cl_2$ (100 mg, 0.199 mmol), **2** (81 mg, 0.442 mmol), and CuI (4 mg, 0.02 mmol). The apparatus was evacuated for 30 min, then argon filled and NEt_3 (5 mL) was added. The lemon-yellow solution was heated to 70 °C and stirred for 19 hours. After cooling to ambient temperature, the solution was filtered and evaporated to dryness in vacuo. The yellow-orange residue was then subject to flash chromatography (basic alumina) using 1:1 EtOAc/hexanes yielded an orange powder (83 mg, 53%). Crystals grown by slow evaporation of a concentrated diethyl ether / pentane solution. ^{1}H NMR ($CDCl_3$, 500 MHz): δ 7.15 – 7.36 (m, 3H, Ar), 2.23 (s, 3H, $NCCH_3$), 2.17 – 2.20 (m, 6H, H1), 1.28 (s, 6H, *gem*-CH_3), 1.20 – 1.27 (m, 9H, H2). $^{13}C\{^1H\}$ NMR ($CDCl_3$, 126 MHz): δ 187.2, 151.2, 145.5, 130.5, 125.8, 123.8, 119.4, 109.8, 107.4 (t, J = 14 Hz), 53.5, 23.2, 16.4 (t, J = 17.6 Hz), 15.4, 8.4. $^{31}P\{^1H\}$ NMR ($CDCl_3$, 243 MHz): δ 11.62 (s). IR (ATR, neat) ν_{max} / cm^{-1}: 2962, 2929, 2873, 2099 (C≡C), 1691, 1609, 1572, 1457, 1417. HRMS (ES(+), MeCN) *m/z*: calcd for $C_{38}H_{55}N_2P_2Pt^+$ $[M+H]^+$ 796.3488, found 796.3510.

12b

Compound was prepared in a similar manner to the above **12**. After evaporation of the reaction solvent, the residue was extracted with benzene and filtered through a small alumina plug. A crystal for XRD studies was grown by diffusion of pentane into a concentrated chloroform solution. ^{1}H NMR ($CDCl_3$, 500 MHz): δ 7.39 (d, J = 8.0 Hz, 1H), 7.23 (dd, J = 1.5, 8.0 Hz, 1H), 7.16 (d, J = 1.5 Hz, 1H), 2.25 (s, 3H, $NCCH_3$), 2.17 – 2.20 (m, 6H), 1.28 (s, 6H, *gem*-CH_3), 1.20 – 1.27 (m, 9H). $^{31}P\{^1H\}$ NMR ($CDCl_3$, 243 MHz): δ 11.13 (s, J = 1188 Hz) (unreferenced).

***trans*-[bis(triphenylphosphine)-bis(5-ethynyl-2,3,3-trimethyl-3*H*-indole)platinum] (13)**

An oven dried and argon filled reflux apparatus was charged with of *cis*-$Pt(PPh_3)_2Cl_2$ (126 mg, 0.159 mmol), **2** (68 mg, 0.371 mmol), and CuI (6 mg, 0.03 mmol). The apparatus was evacuated for 30 min, then dry degassed NH^iPr_2 (15 mL) was added. The yellow solution was heated to reflux and stirred for 3 hours. After cooling to ambient temperature, the solution was filtered and evaporated to dryness in vacuo. The residue was triturated and washed with Et_2O (5 x 2 mL) and EtOH (5 x 2 mL). Further filtration of a CH_2Cl_2 solution and subsequent evaporation gave a pale-yellow precipitate (130 mg, 75%). Crystals grown by slow diffusion of pentane into a concentrated $CDCl_3$ solution. ^{1}H NMR ($CDCl_3$, 500 MHz): δ 7.82 – 7.84 (m, 12H, PPh_3), 7.45 – 7.48 (m, 6H, H4), 7.40 – 7.43 (m, 12H, PPh_3), 7.04 (d, *J* = 7.8 Hz, 2H, H7′), 6.23 (dd, *J* = 1.8 Hz, 7.8 Hz, 2H, H6′), 6.06 (br. s, 2H, H4′), 2.14 (s, 6H, $NCCH_3$), 1.10 (s, 12H, *gem*-CH_3). $^{13}C\{^1H\}$ NMR ($CDCl_3$, 126 MHz): δ 187.5, 151.2, 145.3, 135.4 (t, *J* = 7.5 Hz), 131.9 (t, *J*= 30 Hz), 130.7, 130.1, 128.3 (t, *J* = 4.5 Hz), 125.7, 124.5, 118.8 (C≡C), 113.7 (C≡C), 53.2, 23.2, 15.6. $^{31}P\{^1H\}$ NMR ($CDCl_3$, 243 MHz): δ 19.18 (s). IR (ATR, neat) ν_{max} / cm^{-1}: 2960, 2105 (C≡C), 1573, 1481, 1458, 1434. HRMS (AP(+), MeCN) *m/z*: calcd for $C_{62}H_{55}N_2P_2Pt^+$ $[M+H]^+$ 1084.3488, found 1084.3472.

Dichlorobis(tricyclohexylphospine)platinum, *trans*-[$Pt(PCy_3)_2Cl_2$] (14)

Synthesised by an adapted literature procedure.[56] $(NH_4)_2PtCl_4$ (1.00 g, 2.68 mmol) was added to degassed water in a Schlenk flask. To this was added PCy_3 (7.6 g 20% weight in toluene, 5.4 mmol) dropwise with vigorous stirring. The solution was allowed to stir for 24 h at ambient temperature under argon. The white precipitate was collected by vacuum filtration and washed with water and ethanol and hexanes, then dried in a vacuum desiccator (1.82 g, 83%). The NMR is in agreement to the literature.[103] ^{1}H NMR ($CDCl_3$, 500 MHz): δ 2.60 – 2.65 (m, 3H), 1.64 – 1.98 (m, 20H), 1.22 – 1.30 (m, 10H). $^{31}P\{^1H\}$ NMR ($CDCl_3$, 243 MHz): δ 17.18 (s, *J* = 2398 Hz).

***trans*-[bis(tricyclohexylphosphine)bis(4-ethynylbenzene)platinum] (15)**

Compound **14** (50 mg, 0.061 mmol), and CuI (2 mg) were suspended in $CHCl_3$ (3 mL) and NEt_3 (0.2 mL). Phenylacetylene (0.1 mL, 0.9 mmol) was added and then solution became immediately yellow. The reaction was heated to 55 °C for 11 days. The solution was concentrated, and ethanol was added to precipitate the product. The yellow powder was then recrystallized from $CHCl_3$ and ethanol (34 mg, 58%). ^{1}H NMR (CD_2Cl_2, 500 MHz): δ 7.05 – 7.32 (m, 5H, Ph), 2.87 – 2.91 (m, 3H, Cy), 1.72 – 2.11 (m, 20H), 1.20 – 1.26 (m, 10H). $^{13}C\{^1H\}$ NMR (CD_2Cl_2, 126 MHz): δ 130.8, 128.2, 124.6, 33.9 (t, J = 14.3 Hz), 30.3, 28.2 (t, J = 6.5 Hz), 27.2. $^{31}P\{^1H\}$ NMR (CD_2Cl_2, 202 MHz): δ 24.06 (s, J = 2408 Hz). IR (ATR, neat) ν_{max} / cm^{-1}: 2927, 2848 2099 (C≡C), 1591, 1566, 1484, 1440. HRMS (ES(+), MeCN) *m/z*: calcd for $C_{46}H_{74}NP_2Pt^+$ $[M\text{-}L+MeCN]^+$ 897.4944; found 897.4997, calcd for $C_{52}H_{77}P_2Pt^+$ $[M+H]^+$ 958.5148, found 958.5185.

***trans*-[bis(tricyclohexylphosphine)-bis(5-ethynyl-2,3,3-trimethyl-3*H*-indole)platinum] (16)**

An oven dried and argon filled schlenk tube was charged with $Pt(PCy_3)_2Cl_2$ (100 mg, 0.121 mmol), **2** (81 mg, 0.442 mmol), and CuI (7 mg). The apparatus was evacuated for 30 min, then argon filled and dry $CHCl_3$ (5 mL) and dry NEt_3 (2 mL) were added. The solution was heated to 55 °C and stirred for 3 weeks. After cooling to ambient temperature the solution was evaporated to dryness in vacuo. The residue was then subject to flash chromatography (basic alumina) using 1:1 EtOAc/hexanes yielding orange microcrystals (21 mg, 15%). Crystals grown by slow cooling of a concentrated methanol solution. ^{1}H NMR ($CDCl_3$, 500 MHz): δ 7.34 (d, J = 7.7 Hz, 2H), 7.21 (d, J = 7.7 Hz, 2H), 7.14 (s, 2H), 2.86 – 2.92 (m, 6H), 1.20 – 2.11 (m, 78H). $^{13}C\{^1H\}$ NMR ($CDCl_3$, 126 MHz): δ 186.6, 150.5, 145.2, 129.7, 123.7, 119.2, 58.5, 53.3, 33.5 (t, J = 13 Hz), 29.9, 27.8 (t, J = 5.3), 26.8, 23.2, 18.4, 15.4. $^{31}P\{^1H\}$ NMR ($CDCl_3$, 243 MHz): δ 23.22 (s, J = 2424 Hz). HRMS (ES(+). MeCN) *m/z*: calcd for $C_{62}H_{91}N_2P_2Pt^+$ $[M+H]^+$ 1120.6305, found 1120.6332.

***trans*-[bis(diphenylphosphinoethane)-bis(5-ethynyl-2,3,3-trimethyl-3*H*-indole)ruthenium] (17)**

[Ru(dppe)$_2$Cl]OTf (107 mg, 0.099 mmol), **2** (49 mg, 0.267 mmol) and KO^{t}Bu (36 mg, 0.32 mmol) were charged to an oven dried and argon filled Schlenk tube and placed under high vacuum for 30 min. The Schlenk tube was backfilled with argon, and dry degassed CH_2Cl_2 (10 mL) was added, and the solution was stirred for 4 days at room temperature. The deep red solution was taken to dryness in vacuo. The crude purple residue was triturated and washed with dry Et_2O (2 x 3 mL), CH_3OH (2 x 3 mL) and pentane (3 mL). The residue was dissolved in CH_2Cl_2 and filtered into a new Schlenk tube and evaporate to dryness, yielding a dark red powder (99 mg, 79%). Crystals were grown by diffusion of pentane into a CH_2Cl_2 solution. ^{1}H NMR (C_6D_6, 600 MHz): δ 7.83 (d, *J* = 7.8 Hz, 2H, H7′), 7.51 – 7.76 (m, 16H, PPh_2), 7.25 (dd, *J* = 1.8 Hz, 7.8 Hz, 2H, H6′), 6.94 – 7.02 (m, 24H, PPh_2), 6.85 (d, *J* = 1.8 Hz, 2H, H4′), 2.56 (br. app. s, 8H, dppe), 2.03 (s, 6H, $NCCH_3$), 1.12 (s, 12H, *gem*-CH_3). ^{13}C{^{1}H} NMR (C_6D_6, 100 MHz): δ 184.6, 151.4, 145.8, 137.9 (m), 134.9, 130.3 (t, *J* = 15 Hz, Cα) 129.7, 129.0, 128.3, 128.0, 127.5, 123.8, 120.0, 117.9 (Cβ), 53.3, 31.8 (m, CH_2CH_2-dppe), 23.4 (*gem*-CH_3), 15.2 ($NCCH_3$). ^{31}P{^{1}H} NMR (C_6D_6, 243 MHz): δ 54.35 (s). IR (ATR, neat) ν_{max} / cm^{-1}: 2958, 2048 (C≡C), 1568, 1455, 1430. HRMS (AP(+), MeCN) *m/z*: calcd for $C_{78}H_{73}N_2P_4Ru^+$ $[M+H]^+$ 1263.3768, found 1263.3789.

***trans*-[tetrakis(triethylphosphosphite)-bis(5-ethynyl-2,3,3-trimethyl-3*H*-indole)ruthenium] (18)**

$Ru(P(OEt)_3)_4Cl_2$ (98 mg, 0.117 mmol), **2** (136 mg, 0.742 mmol) and KPF_6 (127 mg, 0.690 mmol) were charged to an oven-dried and argon filled Schlenk tube and placed under high vacuum for 30 min. The Schlenk tube was backfilled with argon, and dry degassed EtOH (5 mL) and dry degassed NH^{i}Pr$_2$ (2 mL) was added, and the solution was stirred for 8 weeks at room temperature. The

brown-to-orange solution was taken to dryness in vacuo. The crude brown oil was triturated with pentane and filtered through cotton wool until the extracts were colourless. This solution was reduced to dryness again by rotary evaporator. Recrystallisation of the extract with slow cooling of a pentane solution afforded light yellow crystals (19 mg, 14%). ^{1}H NMR ($CDCl_3$, 600 MHz): δ 7.27 (s, 2H, Ar), 6.93 – 6.95 (m, 4H, Ar), 4.33 (q, J = 7.2 Hz, 24H, $P(OCH_2CH_3)_3$), 2.22 (s, 6H, $NCCH_3$), 1.23 (s, 12H, *gem*-CH_3) 1.21 (t, J = 7.2 Hz, 36H, $P(OCH_2CH_3)_3$). $^{13}C\{^1H\}$ NMR ($CDCl_3$, 126 MHz): δ 185.5, 149.2, 145.2, 128.8, 123.2, 119.1, 61.0, 53.2, 23.4, 22.5, 16.6, 15.4. $^{31}P\{^1H\}$ NMR ($CDCl_3$, 243 MHz): δ 136.92 (s). IR (ATR, neat) ν_{max} / cm^{-1}: 2974, 2901, 2066 (C≡C), 1609, 1573, 1457. HRMS (ES(+), MeCN) *m/z*: calcd for $C_{37}H_{72}NO_{12}P_4Ru^+$ $[M-L]^+$ 948.3043, found 948.2996, calcd for $C_{38}H_{72}NO_{13}P_4Ru_+$ $[M-L+CO]^+$ 976.2993, found 976.2938.

Electrochemistry

Cyclic voltammetry was performed in 3 mL reaction vials (eDAQ) a glovebox under an argon atmosphere using a Pt working disc electrode (1 mm diameter; eDAQ) and Pt coated Ti rods as the counter and pseudo-reference electrodes (eDAQ). The surface of the working electrode was polished with an alumina paste (0.05 micron alumina powder) on a polishing cloth, rinsed with milliQ water, ethanol and CH_2Cl_2 and dried under a stream of nitrogen before use. Ferrocene (Fc), Decamethylferrocene (Fc*) or Diacetylferrocene (Ac_2Fc) were used as internal standard and all potentials are reported vs the $Fc/[Fc]^+$ couple. Measurements were conducted in CH_2Cl_2 solution containing 0.1 M tetrabutylammonium hexafluorophosphate (Bu_4NPF_6) as the supporting electrolyte. The electrochemical potential within the cell was controlled using a PalmSens EmStat3+ potentiostat and PSTrace software.

Spectroelectrochemistry

All spectroelectrochemical (SEC) measurements were conducted using an OTTLE cell of Hartl design[104] using dry CH_2Cl_2 as the solvent and 0.1 M Bu_4NPF_6 as the supporting electrolyte. For each experiment, the SEC cell was filled with the analyte solution inside a glovebox and sealed before being removed for operation in the spectrometer. UV/Vis/NIR spectra were recorded on an Agilent Cary 5000 spectrometer. IR spectra were recorded on an Agilent Cary 660 FT-IR/NIR spectrometer. The electrochemical potential within the cell was controlled using a PalmSens EmStat3+ potentiostat. For each measurement, the potential was incrementally increased, and a spectrum was recorded at each step.

Crystallography

The X-ray diffraction measurements were carried out at 100 K on an Oxford Diffraction Gemini-R Ultra diffractometer at The University of Western Australia fitted with a MoKα or CuKα radiation source. Following analytical absorption corrections and solution by direct methods, the structures were refined against F2 with full-matrix least-squares using the SHELXL software suite. The .cif files have been deposited at the CCDC 2255621-2255635.

Single-molecule Conductance

We performed scanning tunnelling microscopy break junction (STM-BJ)[105] experiments to determine single-molecule conductance. In these experiments, the Au STM tip is driven into the Au STM substrate to form a metallic contact, and then it is withdrawn at a constant speed (13 nm s^{-1} in this study). As the tip is retracted, the metallic contact thins to a point-contact, having conductance of G_0, which is then ruptured to yield two atomically sharp nanoelectrodes. The experiment is performed in a solution of the target molecule (1 mM in 1,2,5-trichlorobenzene in this study), which can self-assemble in the freshly formed nanogap to fabricate a molecular junction. The tip is further withdrawn so that the junction is stretched to its maximum length, and

eventually ruptured. The tip is then driven again into the substrate and the process is repeated. Data (as G = I/V) is continuously recorded and compiled in statistical 1D conductance histograms and in 2D conductance / electrode separation plots.

A modified commercial instrument (Keysight Technology 5500 SPM) was used in this study. The original electronics were used to apply the junction bias (V) and to drive the piezoelectric actuator. A custom current amplifier based on the design originally introduced by Mészáros *et al*.[106] was used as I/V converter, and the resulting 4-channel data were acquired using a National Instruments DAQ (NI-9215). We used Au/Cr/glass slides (Arrandee) and 99.999+% Au wire (Goodfellow Cambridge) as, respectively, substrate and tip.

ASSOCIATED CONTENT

Supporting Information.

The Supporting Information is available free of charge: Additional electrochemical, crystallography and spectroscopic data for all products. Supplementary material is available online.

Single-molecule data collected at Liverpool are archived at https://datacat.liverpool.ac.uk/2181.

AUTHOR INFORMATION

Corresponding Author

*George A. Koutsantonis

School of Molecular Science, The University of Western Australia, Crawley WA 6009, Australia

Email: george.koutsantonis@uwa.edu.au

Conflicts of interest

There are no conflicts of interest to declare. The authors declare no competing financial interest. The corresponding author is a Co-Editor in Chief of this journal.

Acknowledgements

This research was supported under the Australian Research Council's Discovery Projects funding scheme (Project Numbers DP150104117 and DP200101659). The authors acknowledge the facilities and the scientific and technical assistance of the Australian Microscopy and Microanalysis Research Facility at the Centre for Microscopy, Characterisation, and Analysis, The University of Western Australia, a facility funded by the University, State and Commonwealth Governments. D.C.-M. gratefully acknowledges the School of Physical Sciences Postdoctoral Development Award of the University of Liverpool for financial support. DJ held an Australian RTP scholarship. AV thanks the Royal Society for support (University Research Fellowship URF\R1\191241).

References

[1] Schwab PFH, Smith JR, Michl J. Synthesis and properties of molecular rods. 2. Zig-zag rods. *Chem Rev* 2005; 105 (4): 1197-1279.
[2] McQuade DT, Pullen AE, Swager TM. Conjugated polymer-based chemical sensors. *Chem Rev* 2000; 100 (7): 2537-2574.
[3] Tour JM. Conjugated macromolecules of precise length and constitution. Organic synthesis for the construction of nanoarchitectures. *Chem Rev* 1996; 96 (1): 537-553.
[4] Low PJ. Metal complexes in molecular electronics: progress and possibilities. *Dalton Trans* 2005; (17): 2821-2824.
[5] Long NJ. Organometallic compounds for nonlinear optics - the search for en-light-enment. *Angew Chem Int Ed* 1995; 34 (1): 21-38.
[6] Sala X, Maji S, Bofill R, Garcia-Anton J, Escriche L, Llobet A. Molecular water oxidation mechanisms followed by transition metals: state of the art. *Acc Chem Res* 2014; 47 (2): 504-516.
[7] Wong WY, Ho CL. Organometallic photovoltaics: a new and versatile approach for harvesting solar energy using conjugated polymetallaynes. *Acc Chem Res* 2010; 43 (9): 1246-1256.

[8] Yam VWW. Molecular design of transition metal alkynyl complexes as building blocks for luminescent metal-based materials: Structural and photophysical aspects. *Acc Chem Res* 2002; 35 (7): 555-563.
[9] Tomasik P, Ratajewicz Z, Newkome GR, Strekowski L. The chemistry of heterocylic compounds. Pyridine-metal complexes.: Wiley; 1985.
[10] de Ruiter G, Lahav M, van der Boom ME. Pyridine Coordination Chemistry for Molecular Assemblies on Surfaces. *Acc Chem Res* 2014; 47 (12): 3407-3416.
[11] He ZH, Li HR, Li ZP. Iodine-Mediated Synthesis of 3H-Indoles via Intramolecular Cyclization of Enamines. *J Org Chem* 2010; 75 (13): 4636-4639.
[12] Lim KH, Hiraku O, Komiyama K, Koyano T, Hayashi M, Kam TS. Biologically active indole alkaloids from Kopsia arborea. *J Nat Prod* 2007; 70 (8): 1302-1307.
[13] Kawasaki T, Higuchi K. Simple indole alkaloids and those with a nonrearranged monoterpenoid unit. *Natural Product Reports* 2005; 22 (6): 761-793.
[14] Kam TS, Choo YM. New indole alkaloids from Alstonia macrophylla. *J Nat Prod* 2004; 67 (4): 547-552.
[15] Haque A, Al-Balushi RA, Al-Busaidi IJ, Khan MS, Raithby PR. Rise of conjugated poly-ynes and poly(metalla-ynes): from design through synthesis to structure-property relationships and applications. *Chem Rev* 2018; 118 (18): 8474-8597.
[16] Long NJ, Williams CK. Metal alkynyl σ-complexes: synthesis and materials. *Angew Chem Int Ed* 2003; 42 (23): 2586-2617.
[17] Bruce MI, Ellis BG, Gaudio M, Lapinte C, Melino G, Paul F, Skelton BW, Smith ME, Toupet L, White AH. Preparation, structures and some reactions of novel diynyl complexes of iron and ruthenium. *Dalton Trans* 2004; (10): 1601-1609.
[18] Miller-Clark LA, Ren T. Syntheses and material applications of Ru(II)(bisphosphine)$_2$ alkynyls. *J Organomet Chem* 2021; 951.
[19] Koutsantonis GA, Jenkins GI, Schauer PA, Szczepaniak B, Skelton BW, Tan C, White AH. Coordinating tectons: bipyridyl-terminated group 8 alkynyl complexes. *Organometallics* 2009; 28 (7): 2195-2205.
[20] Koutsantonis GA, Low PJ, Mackenzie CFR, Skelton BW, Yufit DS. Coordinating tectons: bimetallic complexes from bipyridyl terminated group 8 alkynyl complexes. *Organometallics* 2014; 33 (18): 4911-4922.
[21] Cifuentes MP, Humphrey MG, Koutsantonis GA, Lengkeek NA, Petrie S, Sanford V, Schauer PA, Skelton BW, Stranger R, White AH. Coordinating tectons: Bipyridyl terminated allenylidene complexes. *Organometallics* 2008; 27 (8): 1716-1726.
[22] Schauer PA, Skelton BW, Koutsantonis GA. Coordinating tectons 4: coordination chemistry of the 4,5-diazafluoren-9-yl moiety as a metallo-ligand for allenylidene complexes. *Organometallics* 2015; 34 (20): 4975-4988.
[23] Bock S, Mackenzie CF, Skelton BW, Byrne LT, Koutsantonis GA, Low PJ. Clusters as ligands: synthesis, structure and coordination chemistry of ruthenium clusters derived from 4-and 5-ethyny1-2,2'-bipyridine. *J Organomet Chem* 2016; 812: 190-196.
[24] Rodriguez JG, Urrutia A, de Diego JE, Martinez-Alcazar MP, Fonseca I. Synthesis of 2'-alkylspiro[2-X-cyclohexan-1,3'-3' H-indole] (X = H; X = CH_3) by an unexpected reaction between an organomagnesium halide and 2'-methylspiro[2-X-cyclohexan-1,3'-3'H-indole]. X-ray structure of a fluorescent dimeric compound. *J Org Chem* 1998; 63 (13): 4332-4337.

[25] Rodriguez JG, Urrutia A. Synthesis of sterically hindered 4a,9a-disubstituted 1,2,3,4,4a,9a-hexahydrocarbazoles from 4a-methyl-1,2,3,4-tetrahydro-4aH-carbazole with organolithium reagents. *Tetrahedron* 1998; 54 (51): 15613-15618.
[26] Fehlner JR, Borowski PJ, Pettinato PL, Freyer AJ. Condensation of 2,3,3-trimethyl-3H-Indole with methylene iodide and oxidative coupling. *J Org Chem* 1984; 49 (1): 170-172.
[27] Kanaoka Y, Miyashita K, Yonemitsu O. 3H-Indoles. IV. Photo-and peroxide-induced oxygenation of 2-ethyl-3H-indoles. *Chemical and Pharmaceutical Bulletin* 1970; 18 (3): 634-637.
[28] Kanaoka Y, Miyashita K, Yonemitsu O. 3H-indoles—II: Synthesis of 3-alkyl-3H-indoles by the alkylation of 2,3-disubstituted indoles with polyphosphate ester and some reactions of the 3H-indole system. *Tetrahedron* 1969; 25 (14): 2757-2766.
[29] Liu SY, Zhang WZ, Qu JP, Wang BM. Engaging 2-methyl indolenines in a tandem condensation/1,5-hydride transfer/cyclization process: construction of a novel indolenine-tetrahydroquinoline assembly. *Organic Chemistry Frontiers* 2018; 5 (20): 3008-3012.
[30] Wang QC, Qu DH, Ren J, Xu LH, Liu MY, Tian H. New benzo[e]indolinium cyanine dyes with two different fluorescence wavelengths. *Dyes Pigm* 2003; 59 (2): 163-172.
[31] Shachkus AA, Degutite RY. Reaction of 2,3,3-trimethyl-3H-indole salts with acrylamide. Synthesis of 1,2,3,4,10,10a-hexahydropyrimido[1,2-a]indol-2-one derivatives. *Chem Heterocycl Compd* 1986; 22 (8): 852-855.
[32] Bruce M, Koutsantonis G. Cyclopentadienyl-ruthenium and -osmium chemistry. XXXV. Some ethynyl, vinylidene and related complexes. *Aust J Chem* 1991; 44 (2): 207-217.
[33] Sonogashira K, Yatake T, Tohda Y, Takahashi S, Hagihara N. Novel preparation of σ-alkynyl complexes of transition metals by copper(I) iodide-catalysed dehydrohalogenation. *J Chem Soc, Chem Commun* 1977; (9): 291-292.
[34] Vicente J, Gil-Rubio J, Barquero N, Jones PG, Bautista D. Synthesis of luminescent alkynyl gold metalaligands containing 2,2'-bipyridine-5-yl and 2,2': 6',2''-terpyridine-4-yl donor groups. *Organometallics* 2008; 27 (4): 646-659.
[35] Khairul WM, Fox MA, Zaitseva NN, Gaudio M, Yufit DS, Skelton BW, White AH, Howard JAK, Bruce MI, Low PJ. Transition metal alkynyl complexes by transmetallation from Au(CCAr)(PPh_3) (Ar = C_6H_5 or C_6H_4Me-4). *Dalton Trans* 2009; (4): 610-620.
[36] Rudolph M, Hashmi ASK. Gold catalysis in total synthesis-an update. *Chem Soc Rev* 2012; 41 (6): 2448-2462.
[37] Leyva-Perez A, Domenech A, Al-Resayes SI, Corma A. Gold redox catalytic cycles for the oxidative coupling of alkynes. *ACS Catal* 2012; 2 (1): 121-126.
[38] Fox MA, Roberts RL, Khairul WM, Hartl F, Low PJ. Spectroscopic properties and electronic structures of 17-electron half-sandwich ruthenium acetylide complexes, $[Ru(CCAr)(L\text{-}2)Cp']^+$ (Ar = phenyl, p-tolyl, 1-naphthyl, 9-anthryl; L-2=$(PPh_3)_2$, Cp'=Cp; L-2=dppe; Cp'=Cp*). *J Organomet Chem* 2007; 692 (15): 3277-3290.
[39] Harrison DP, Kumar VJ, Noppers JN, Gluyas JBG, Sobolev AN, Moggach SA, Low PJ. Iron vs. ruthenium: syntheses, structures and IR spectroelectrochemical characterisation of half-sandwich Group 8 acetylide complexes. *New J Chem* 2021; 45 (33): 14932-14943.
[40] Whittall IR, Humphrey MG, Hockless DCR, Skelton BW, White AH. Organometallic complexes for nonlinear optics. 2. Syntheses, electrochemical studies, structural characterization, and computationally-derived molecular quadratic hyperpolarizabilities of ruthenium σ-arylacetylides: X-ray crystal structures of Ru(CCPh)(PMe_3)$_2$(C_5H_5) and Ru($CCC_6H_4NO_2$-4)(L)2(C_5H_5) (L = PPh_3, PMe_3). *Organometallics* 1995; 14 (8): 3970-3979.

[41] Mackenzie CFR, Bock S, Lim CY, Skelton BW, Nervi C, Wild DA, Low PJ, Koutsantonis GA. Coordinating tectons. Experimental and computational infrared data as tools to identify conformational isomers and explore electronic structures of 4-ethynyl-2,2'-bipyridine complexes. *Organometallics* 2017; 36 (10): 1946-1961.
[42] Whittall IR, Humphrey MG, Houbrechts S, Persoons A, Hockless DCR. Organometallic complexes for nonlinear Optics. 8.1 Syntheses and molecular quadratic hyperpolarizabilities of systematically varied (triphenylphosphine)gold σ-srylacetylides: X-ray crystal structures of $Au(CCR)(PPh_3)$ (R = 4-$C_6H_4NO_2$, 4,4‘-$C_6H_4C_6H_4NO_2$). *Organometallics* 1996; 15 (26): 5738-5745.
[43] Bruce MI, Swincer AG, Wallis RC. Cyclopentadienyl-ruthenium and cyclopentadienyl-osmium chemistry - Some reactions of substituted vinylidene complexes. *J Organomet Chem* 1979; 171 (1): C5-C8.
[44] Fox MA, Harris JE, Heider S, Pérez-Gregorio V, Zakrzewska ME, Farmer JD, Yufit DS, Howard JAK, Low PJ. A simple synthesis of trans-$RuCl(CCR)(dppe)_2$ complexes and representative molecular structures. *J Organomet Chem* 2009; 694 (15): 2350-2358.
[45] Packheiser R, Ecorchard P, Walfort B, Lang H. Heterotrimetallic and heterotetrametallic transition metal complexes. *J Organomet Chem* 2008; 693 (6): 933-946.
[46] Paul F, Ellis BG, Bruce MI, Toupet L, Roisnel T, Costuas K, Halet JF, Lapinte C. Bonding and substituent effects in electron-rich mononuclear ruthenium sigma-arylacetylides of the formula $[(dppe)(C_5Me_5)Ru(CC)\text{-}1,4\text{-}(C_6H_4)X][PF_6]_n$ (n = 0, 1; X = NO_2, CN, F, H, OMe, NH_2). *Organometallics* 2006; 25 (3): 649-665.
[47] Wu IY, Lin JT, Luo J, Sun SS, Li CS, Lin KJ, Tsai CT, Hsu CC, Lin JL. Syntheses and reactivity of ruthenium σ-pyridylacetylides. *Organometallics* 1997; 16 (10): 2038-2048.
[48] Ge Q, Hor TSA. Stepwise assembly of linearly-aligned Ru–M–Ru (M = Pd, Pt) heterotrimetallic complexes with σ-4-ethynylpyridine spacer. *Dalton Trans* 2008; (22): 2929-2936.
[49] D'Amato R, Furlani A, Colapietro M, Portalone G, Casalboni M, Falconieri M, Russo MV. Synthesis, characterisation and optical properties of symmetrical and unsymmetrical Pt(II) and Pd(II) bis-acetylides. Crystal structure of trans-$[Pt(PPh_3)_2(CC–C_6H_5)(CC–C_6H_4NO_2)]$. *J Organomet Chem* 2001; 627 (1): 13-22.
[50] Sonogashira K, Fujikura Y, Yatake T, Toyoshima N, Takahashi S, Hagihara N. Syntheses and properties of *cis*- and *trans*-dialkynyl complexes of platinum(II). *J Organomet Chem* 1978; 145 (1): 101-108.
[51] Xu H-B, Ni J, Chen K-J, Zhang L-Y, Chen Z-N. Preparation, characterization, and photophysical Properties of *cis*- or *trans*-$PtLn_2$ (Ln = Nd, Eu, Yb) arrays with 5-ethynyl-2,2′-bipyridine. *Organometallics* 2008; 27 (21): 5665-5671.
[52] Gimeno A, Rodríguez-Gimeno A, Cuenca AB, Ramírez de Arellano C, Medio-Simón M, Asensio G. Gold(I)-catalysed cascade reactions in the synthesis of 2,3-fused indole derivatives. *Chem Commun* 2015; 51 (62): 12384-12387.
[53] Takani M, Masuda H, Yamauchi O. Palladium(II) complex formation by indole-3-acetate. Mixed ligand complexes involving a unique spiro-ring formed by cyclopalladation. *Inorg Chim Acta* 1995; 235 (1): 367-374.
[54] Takani M, Takeda T, Yajima T, Yamauchi O. Indole rings in palladium(II) complexes. Dual mode of metal binding and aromatic ring stacking causing *syn−anti* isomerism. *Inorg Chem* 2006; 45 (15): 5938-5946.

[55] Barrett BJ, Iluc VM. An adaptable chelating diphosphine ligand for the stabilization of palladium and platinum carbenes. *Organometallics* 2017; 36 (3): 730-741.
[56] Al-Owaedi OA, Bock S, Milan DC, Oerthel MC, Inkpen MS, Yufit DS, Sobolev AN, Long NJ, Albrecht T, Higgins SJ, Bryce MR, Nichols RJ, Lambert CJ, Low PJ. Insulated molecular wires: Inhibiting orthogonal contacts in metal complex based molecular junctions. *Nanoscale* 2017; 9 (28): 9902-9912.
[57] Schull TL, Kushmerick JG, Patterson CH, George C, Moore MH, Pollack SK, Shashidhar R. Ligand effects on charge transport in platinum(II) acetylides. *J Am Chem Soc* 2003; 125 (11): 3202-3203.
[58] Touchard D, Haquette P, Guesmi S, LePichon L, Daridor A, Toupet L, Dixneuf PH. Vinylidene-, alkynyl-, and trans-bis(alkynyl)ruthenium complexes. Crystal structure of trans-[Ru(NH3)(C C-Ph)(Ph2PCH2CH2PPh2)(2)]PF6. *Organometallics* 1997; 16 (16): 3640-3648.
[59] Touchard D, Morice C, Cadierno V, Haquette P, Toupet L, Dixneuf PH. Novel Allenylidene Alkynyl and Ammonia Alkynyl Metal-Complexes Via Selective Synthesis of Mono and Bis Alkynyl Ruthenium(Ii) Complexes - Crystal-Structure of Trans-[Ru(Nh3)(C-Equivalent-to-Cph)(Ph2pch2ch2pph2)2]Pf6. *J Chem Soc Chem Comm* 1994; (7): 859-860.
[60] Naher M, Bock S, Langtry ZM, O'Malley KM, Sobolev AN, Skelton BW, Korb M, Low PJ. Synthesis, structure and physical properties of "wire-like" metal complexes. *Organometallics* 2020; 39 (24): 4667-4687.
[61] Eaves SG, Skelton BW, Low PJ. Syntheses and molecular structures of *trans*-bis(alkynyl) tetrakis-triethylphosphite ruthenium complexes. *J Organomet Chem* 2017; 847: 242-250.
[62] Albertin G, Autoniutti S, Bordignon E, Cazzaro F, Ianelli S, Pelizzi G. Preparation, structure, and reactivity of new bis(acetylide) and acetylide-vinylidene Ruthenium(II) complexes stabilized by phosphite ligands. *Organometallics* 1995; 14 (9): 4114-4125.
[63] Marqués-González S, Parthey M, Yufit DS, Howard JAK, Kaupp M, Low PJ. Combined spectroscopic and quantum chemical study of [*trans*-$Ru(CCC_6H_4R^1\text{-}4)_2(dppe)_2]^{n+}$ and [*trans*-$Ru(CCC_6H_4R^1\text{-}4)(CCC_6H_4R^2\text{-}4)(dppe)_2]^{n+}$ (n = 0, 1) complexes: Interpretations beyond the lowest energy conformer paradigm. *Organometallics* 2014; 33 (18): 4947-4963.
[64] Bryce MR. A review of functional linear carbon chains (oligoynes, polyynes, cumulenes) and their applications as molecular wires in molecular electronics and optoelectronics. *J Mater Chem C* 2021.
[65] Casari CS, Tommasini M, Tykwinski RR, Milani A. Carbon-atom wires: 1-D systems with tunable properties. *Nanoscale* 2016; 8 (8): 4414-4435.
[66] Liu J, Lam JWY, Tang BZ. Acetylenic polymers: syntheses, structures, and functions. *Chem Rev* 2009; 109 (11): 5799-5867.
[67] Hay AS. Oxidative coupling of acetylenes. III. *J Org Chem* 1962; 27 (9): 3320-3321.
[68] Eglinton G, Galbraith AR. 182. Macrocyclic acetylenic compounds. Part I. Cyclotetradeca-1 :3-diyne and related compounds. *J Chem Soc (Resumed)* 1959: 889-896.
[69] Glaser C. Untersuchungen über einige Derivate der Zimmtsäure. *Justus Liebigs Ann Chem* 1870; 154 (2): 137-171.
[70] Batsanov AS, Collings JC, Fairlamb IJS, Holland JP, Howard JAK, Lin Z, Marder TB, Parsons AC, Ward RM, Zhu J. Requirement for an oxidant in Pd/Cu co-catalyzed terminal alkyne homocoupling to give symmetrical 1,4-disubstituted 1,3-diynes. *J Org Chem* 2005; 70 (2): 703-706.
[71] Younus M, Long NJ, Raithby PR, Lewis J. Synthetic, spectroscopic and electrochemical characterisation of mixed-metal acetylide complexes. *J Organomet Chem* 1998; 570 (1): 55-62.

[72] Masai H, Sonogash.K, Hagihara N. Electronic spectra of square-planar bis(tertiary phosphine)dialkynyl complexes of nickel(II), palladium(II), and platinum(II). *Bull Chem Soc Jpn* 1971; 44 (8): 2226-+.
[73] Choi MY, Chan MCW, Zhang SB, Cheung KK, Che CM, Wong KY. MLCT and LMCT transitions in acetylide complexes. Structural, spectroscopic, and redox properties of ruthenium(II) and -(III) bis(sigma-arylacetylide) complexes supported by a tetradentate macrocyclic tertiary amine ligand. *Organometallics* 1999; 18 (11): 2074-2080.
[74] Wong CY, Che CM, Chan MCW, Han J, Leung KH, Phillips DL, Wong KY, Zhu NY. Probing ruthenium-acetylide bonding interactions: Synthesis, electrochemistry, and spectroscopic studies of acetylide-ruthenium complexes supported by tetradentate macrocyclic amine and diphosphine ligands. *J Am Chem Soc* 2005; 127 (40): 13997-14007.
[75] Powell CE, Cifuentes MP, McDonagh AM, Hurst SK, Lucas NT, Delfs CD, Stranger R, Humphrey MG, Houbrechts S, Asselberghs I, Persoons A, Hockless DCR. Organometallic complexes for nonlinear optics. Part 27. Syntheses and optical properties of some iron, ruthenium and osmium alkynyl complexes. *Inorg Chim Acta* 2003; 352: 9-18.
[76] Powell CE, Cifuentes MP, Morrall JP, Stranger R, Humphrey MG, Samoc M, Luther-Davies B, Heath GA. Organometallic complexes for nonlinear optics. 30. Electrochromic linear and nonlinear optical properties of alkynylbis(diphosphine)ruthenium complexes. *J Am Chem Soc* 2003; 125 (2): 602-610.
[77] Holliman PJ, Horton PN, Hursthouse MB. CCDC 1011855: Experimental crystal structure determination. 2014.
[78] de Aquino A, Caparros FJ, Aullon G, Ward JS, Rissanen K, Jung Y, Choi H, Lima JC, Rodriguez L. Effect of Gold(I) on the Room-Temperature Phosphorescence of Ethynylphenanthrene. *Che Eur J* 2021; 27 (5): 1810-1820.
[79] Hurst SK, Lucas NT, Humphrey MG, Isoshima T, Wostyn K, Asselberghs I, Clays K, Persoons A, Samoc M, Luther-Davies B. Organometallic complexes for nonlinear optics. Part 29. Quadratic and cubic hyperpolarizabilities of stilbenylethynyl-gold and -ruthenium complexes. *Inorg Chim Acta* 2003; 350: 62-76.
[80] Khairul WM, Albesa-Jove D, Yufit DS, Al-Haddad MR, Collings JC, Hartl F, Howard JAK, Marder TB, Low PJ. The syntheses, structures and redox properties of phosphine-gold(I) and triruthenium-carbonyl cluster derivatives of tolans. *Inorg Chim Acta* 2008; 361 (6): 1646-1658.
[81] Khairul WM, Porres L, Albesa-Jove D, Senn MS, Jones M, Lydon DP, Howard JAK, Beeby A, Marder TB, Low PJ. Metal cluster terminated "molecular wires". *J Cluster Sci* 2006; 17 (1): 65-85.
[82] González MT, Zhao X, Manrique DZ, Miguel D, Leary E, Gulcur M, Batsanov AS, Rubio-Bollinger G, Lambert CJ, Bryce MR, Agraït N. Structural versus electrical functionalization of oligo(phenylene ethynylene) diamine molecular junctions. *J Phys Chem C* 2014; 118 (37): 21655-21662.
[83] Gagnon K, Mohammed Aly S, Brisach-Wittmeyer A, Bellows D, Bérubé J-F, Caron L, Abd-El-Aziz AS, Fortin D, Harvey PD. Conjugated oligomers and polymers of *cis*- and *trans*-platinum(II)-*para*- and *ortho*-bis(ethynylbenzene)quinone diimine. *Organometallics* 2008; 27 (10): 2201-2214.
[84] Mayor M, von Hänisch C, Weber HB, Reichert J, Beckmann D. A *trans*-platinum(II) complex as a single-molecule insulator. *Angew Chem Int Ed* 2002; 41 (7): 1183-1186.

[85] Parthey M, Vincent KB, Renz M, Schauer PA, Yufit DS, Howard JAK, Kaupp M, Low PJ. A combined computational and spectroelectrochemical study of platinum-bridged *bis*-triarylamine systems. *Inorg Chem* 2014; 53 (3): 1544-1554.
[86] Ravera M, D'Amato R, Guerri A. Probing delocalisation across highly ethynylated mono and dinuclear Pt(II) tethers containing nitrogroups and organic models as redox active probes: X-ray crystal structure of *trans*-[Pt(CC–$C_6H_4NO_2$)$_2$(PPh_3)$_2$]. *J Organomet Chem* 2005; 690 (9): 2376-2380.
[87] Vicente J, Chicote M-T, Alvarez-Falcón MM, Jones PG. Platinum(II) and mixed platinum(II)/gold(I) σ-alkynyl complexes. The first Anionic σ-alkynyl metal polymers. *Organometallics* 2005; 24 (11): 2764-2772.
[88] Zhou G, Wong W-Y, Poon S-Y, Ye C, Lin Z. Symmetric versus unsymmetric platinum(II) bis(aryleneethynylene)s with distinct electronic structures for optical power limiting/optical transparency trade-off optimization. *Adv Funct Mater* 2009; 19 (4): 531-544.
[89] Hong W, Manrique DZ, Moreno-García P, Gulcur M, Mishchenko A, Lambert CJ, Bryce MR, Wandlowski T. Single molecular conductance of tolanes: Experimental and theoretical study on the junction evolution dependent on the anchoring group. *J Am Chem Soc* 2012; 134 (4): 2292-2304.
[90] Bock S, Al-Owaedi OA, Eaves SG, Milan DC, Lemmer M, Skelton BW, Osorio HM, Nichols RJ, Higgins SJ, Cea P, Long NJ, Albrecht T, Martín S, Lambert CJ, Low PJ. Single-molecule conductance studies of organometallic complexes bearing 3-thienyl contacting groups. *Chem Eur J* 2017; 23 (9): 2133-2143.
[91] González MT, Díaz A, Leary E, García R, Herranz MÁ, Rubio-Bollinger G, Martín N, Agraït N. Stability of single- and few-molecule junctions of conjugated diamines. *J Am Chem Soc* 2013; 135 (14): 5420-5426.
[92] Velizhanin KA, Zeidan TA, Alabugin IV, Smirnov S. Single molecule conductance of bipyridyl ethynes: the role of surface binding modes. *J Phys Chem B* 2010; 114 (45): 14189-14193.
[93] Quek SY, Kamenetska M, Steigerwald ML, Choi HJ, Louie SG, Hybertsen MS, Neaton JB, Venkataraman L. Mechanically controlled binary conductance switching of a single-molecule junction. *Nature Nanotech* 2009; 4 (4): 230-234.
[94] Moreno-García P, Gulcur M, Manrique DZ, Pope T, Hong W, Kaliginedi V, Huang C, Batsanov AS, Bryce MR, Lambert C, Wandlowski T. Single-molecule conductance of functionalized oligoynes: Length dependence and junction evolution. *J Am Chem Soc* 2013; 135 (33): 12228-12240.
[95] Gulcur M, Moreno-García P, Zhao X, Baghernejad M, Batsanov AS, Hong W, Bryce MR, Wandlowski T. The synthesis of functionalised diaryltetraynes and their transport properties in single-molecule junctions. *Chem Eur J* 2014; 20 (16): 4653-4660.
[96] Skipper HE, May CV, Rheingold AL, Doerrer LH, Kamenetska M. Hard-Soft Chemistry Design Principles for Predictive Assembly of Single Molecule-Metal Junctions. *J Am Chem Soc* 2021; 143 (40): 16439-16447.
[97] Low PJ, Bock S. Spectroelectrochemistry: A valuable tool for the study of organometallic-alkyne, -vinylidene, -cumulene, -alkynyl and related complexes. *Electrochim Acta* 2013; 110: 681-692.
[98] Fox MA, Le Guennic B, Roberts RL, Brue DA, Yufit DS, Howard JAK, Manca G, Halet JF, Hartl F, Low PJ. Simultaneous bridge-localized and mixed-valence character in diruthenium

radical cations featuring diethynylaromatic bridging ligands. *J Am Chem Soc* 2011; 133 (45): 18433-18446.
[99] Gluyas JBG, Brown NJ, Farmer JD, Low PJ. Optimised syntheses of the half-sandwich complexes FeCl(dppe)Cp*, FeCl(dppe)Cp, RuCl(dppe)Cp*, and RuCl(dppe)Cp. *Aust J Chem* 2017; 70 (1): 113-119.
[100] Bruce MI, Hameister C, Swincer AG, Wallis RC, Ittel SD. Chloro(η^5-cyclopentadienyl)bis(triphenyl-phosphine) ruthenium(II): $RuCl(PPh_3)_2(C_5H_5)$. *Inorg Synth* 1990; 28: 270-272.
[101] McAuliffe CA, Parish RV, Randall PD. Gold(I) complexes of unidentate and bidentate phosphorus-, arsenic-, antimony-, and sulphur-donor ligands. *J Chem Soc, Dalton Trans* 1979; (11): 1730-1735.
[102] Eisenstadt A, Tannenbaum R, Efraty A. Convenient synthetic routes to the cyclopentadienylruthenium dicarbonyl chloride and bromide. *J Organomet Chem* 1981; 221 (3): 317-321.
[103] Al-Najjar IM. ^{31}P and ^{195}Pt NMR characteristics of new binuclear complexes of $[Pt_2X_4](PR_3)_2$] *cis*/*trans* isomers and of mononuclear analogs. *Inorg Chim Acta* 1987; 128 (1): 93-104.
[104] Krejcik M, Danek M, Hartl F. Simple Construction of an Infrared Optically Transparent Thin-Layer Electrochemical-Cell - Applications to the Redox Reactions of Ferrocene, Mn2(Co)10 and Mn(Co)3(3,5-Di-Tert-Butyl-Catecholate)-. *J Electroanal Chem* 1991; 317 (1-2): 179-187.
[105] Xu BQ, Tao NJJ. Measurement of single-molecule resistance by repeated formation of molecular junctions. *Science* 2003; 301 (5637): 1221-1223.
[106] Meszaros G, Li C, Pobelov I, Wandlowski T. Current measurements in a wide dynamic range - applications in electrochemical nanotechnology. *Nanotechnology* 2007; 18 (42).